

DOCUMENT ROOM ~~DOCUMENT ROOM 36-412~~  
RESEARCH LABORATORY OF ELECTRONICS  
MASSACHUSETTS INSTITUTE OF TECHNOLOGY

COPY # 3

CHARACTERIZATION OF PROBABILITY DISTRIBUTIONS  
FOR EXCESS PHYSICAL NOISES

JACK HILIBRAND

FOR LOAN ONLY

TECHNICAL REPORT 276

SEPTEMBER 7, 1956

RESEARCH LABORATORY OF ELECTRONICS  
MASSACHUSETTS INSTITUTE OF TECHNOLOGY  
CAMBRIDGE, MASSACHUSETTS

The Research Laboratory of Electronics is an interdepartmental laboratory of the Department of Electrical Engineering and the Department of Physics.

The research reported in this document was made possible in part by support extended the Massachusetts Institute of Technology, Research Laboratory of Electronics, jointly by the U. S. Army (Signal Corps), the U. S. Navy (Office of Naval Research), and the U. S. Air Force (Office of Scientific Research, Air Research and Development Command), under Signal Corps Contract DA36-039-sc-64637, Department of the Army Task 3-99-06-108 and Project 3-99-00-100.

MASSACHUSETTS INSTITUTE OF TECHNOLOGY  
RESEARCH LABORATORY OF ELECTRONICS

Technical Report 276

September 7, 1956

CHARACTERIZATION OF PROBABILITY DISTRIBUTIONS FOR EXCESS  
PHYSICAL NOISES

Jack Hilibrand

This report is based on a thesis that was submitted to the Department of Electrical Engineering, August 1956, in partial fulfillment of the requirements for the degree of Doctor of Science, Massachusetts Institute of Technology.

ABSTRACT

Theoretical and experimental techniques are described for characterizing the probability distributions of certain excess physical noises by their moments. Theoretical methods are presented for applying this "moments technique" in the time domain to random-pulse noise, and in the frequency domain to any random functions for which the moments exist. The frequency-domain technique is used for a theoretical study of the approach to a gaussian distribution of random-pulse noise that is subjected to severe band-limiting. In contrast, the departure from a gaussian distribution of random-pulse noise that is band-limited by RC cutoffs at low and high frequencies is examined by using the time-domain technique. It is found that the approach of noise distributions to gaussian is governed by the "memory" of the filter system rather than simply by its bandwidth.

An experimental system is described for measuring the first four moments of noises in the 0.2 cps - 10 kc range. It is concluded that experimental measurements of moments are more desirable than direct probability density measurements when the goals are: (a) to categorize broadly the form of continuous noise distribution by a small number of parameters, and/or (b) when a minimum investment of time and equipment is desired.

Measurements on  $1/f$  noise in germanium diodes confirm (within experimental error) that the first probability distribution of this noise is gaussian in nature. Some effects of limited system bandwidth are illustrated by measurements on the distinctly non-gaussian "avalanche" noise in silicon junction diodes.



## Table of Contents

	Page
I. Introduction	1
Excess Physical Noise	1
Noise Amplitude Distributions of Non-Gaussian Noises	1
Measurement of Amplitude Distributions	2
Results of this Investigation	2
II. The Moments Technique for Use in the Frequency Domain	4
Significance of Moments in Evaluating Amplitude Distributions	4
Evaluation of the Moments in the Frequency Domain	5
Evaluation of the Moments in the Time Domain for Random-Pulse Noise	9
III. Some Applications of the Moments Technique	12
Evaluation of the Higher-Order Power Spectra for Random-Pulse Noise	12
The Approach to a Gaussian Distribution of Filtered Random-Pulse Noise: An Application of the Moments Technique in the Frequency Domain	17
The Effect of Low-Frequency Filtering on Random-Pulse Noise: An Application of the Moments Technique in the Time Domain	22
IV. Semiconductor Noise Measurements	25
Measurements and Techniques	25
Errors Resulting from Length of Observation Time	27
Errors Resulting from a Limited Amplitude Range	31
Measurements of $1/f$ Excess Noise	33
Avalanche Noise	34
V. Conclusions	45
Acknowledgment	46
Appendix: Further Applications of the Moments Approach in the Time Domain	47
Bibliography	50



## I. INTRODUCTION

### 1.1 EXCESS PHYSICAL NOISE

The noises that appear in electronic devices have been classified as thermal noise arising from statistical fluctuations of the thermal energy of the device, shot noise arising from the discrete nature of the electron, and excess physical noise (1), which includes all of the noises that derive from the particular physical structure of the material, and which is usually ascribable to conductivity fluctuations. Some examples of excess physical noises are the  $1/f$  noise in semiconductors, avalanche noise in the reverse breakdown of semiconductor diodes, and flicker noise in vacuum tubes. In this work the first-order amplitude probability density of  $1/f$  semiconductor noise and of avalanche noise were investigated experimentally. We shall assume that the reader is acquainted with the standard results in noise theory, such as those that can be found in reference 12.

Direct measurement of the first probability density is difficult for physical noises that have a  $1/f$  spectral density, since this spectrum leads to long correlation times and, therefore, to long observation times and elaborate data collection systems. Filtering the low-frequency components of the noise to decrease the correlation time, however, can modify the probability distribution considerably. It is for this reason that we have used a technique of measuring moments for the purpose of evaluating the probability distribution, rather than measuring the distribution density directly. Since one purpose of these measurements is to establish experimentally the gaussian or non-gaussian nature of semiconductor  $1/f$  excess noise, proof is included that for a wide class of non-gaussian noise models, RC limiting of the low-frequency portion of the spectrum leads to an increasing deviation from a gaussian distribution. Studies undertaken for avalanche noise (which is markedly non-gaussian) illustrate some of the effects of filtering on the probability distribution that is to be measured.

### 1.2 NOISE AMPLITUDE DISTRIBUTIONS OF NON-GAUSSIAN NOISES

Two classes of non-gaussian noises have received attention recently: noise derived from gaussian by a resistive nonlinearity and noise resulting from the superposition of independent pulses.

In the past decade work has been done by Rice, Bennett, Middleton, and others (2), in examining the effect of a resistive nonlinear system on the probability distribution and spectral density of a gaussian noise input. The general problem of the effect of resistive nonlinearities on amplitude distributions of all orders is susceptible of immediate solution; therefore attention was focused on mathematical techniques for the evaluation of the power spectrum. Solution for the probability distribution in the case of nonlinearities with energy storage was accomplished, for a square-law detector followed by filtering, by Kac and Siegert (3), but other detector characteristics have not been treated analytically.

Random-pulse noise, which has been investigated by Rice and Middleton (4), provides a field in which application of the moments technique is straightforward. This report is devoted primarily to examination of pulse noise, although the methods used can be applied more generally (9).

### 1.3 MEASUREMENT OF AMPLITUDE DISTRIBUTIONS

Early measurements (5) of probability distributions were made by inspection of photographic records of the waveforms under investigation. The accuracy of the results obtained by this method was usually limited by the length of the analyzed time interval, which, in turn, was limited by the laboriousness and time-consuming nature of the measurements. Later techniques have been based either on the use of electronic level selectors or on measurements made with cathode-ray tube displays (6). The electronic-selector technique, when combined with digital counting schemes, can provide measurements over the long periods needed for the tails of the distribution, but it requires extensive and complicated equipment. Measurements with cathode-ray tube displays and photocells are limited by the integrator time constant to moderate lengths of observation time. If photographic techniques are used to examine the display, the time of observation can be extended considerably, but the numerical evaluation of the probability density is quite difficult.

We have no specific knowledge, at this time, of any instance of the use of measurements of moments to evaluate waveform probability distributions, but the widespread use of this technique in statistical and actuarial work leads us to suppose that its application to (electrical) waveforms must have at least been contemplated by others.

### 1.4 RESULTS OF THIS INVESTIGATION

In this report analytic methods for evaluating the moments of a probability distribution after filtering by using either a time-domain or frequency-domain approach are provided, together with examples of their application. A proof of the approach to a gaussian distribution for random-pulse noises, which are examined after severe band-limiting, is given. Attention in this proof is centered on the nature of the approach to a gaussian distribution as the bandwidth is decreased. In contrast, the effect of RC filtering of the low end of the random-pulse noise spectral density is found to be an increasing departure from a gaussian distribution, and consideration of this case leads to a clarification of the concept of band-limiting which is implied in such a statement as "under band-limiting non-gaussian noises tend toward a gaussian distribution."

Equipment which has been used to measure moments experimentally is described briefly and the conditions under which experimental use of the method of moments is most desirable are discussed. The results of measurements on  $1/f$  noise from a



germanium junction diode and on avalanche noise in silicon junction diodes are given. Some of the effects of a limited-system bandwidth on measurements of a non-gaussian distribution are shown by the results for filtered avalanche noise.

## II. THE MOMENTS TECHNIQUE FOR USE IN THE FREQUENCY DOMAIN AND TIME DOMAIN

### 2.1 SIGNIFICANCE OF MOMENTS IN EVALUATING AMPLITUDE DISTRIBUTIONS

In this section we shall show how the values of the moments define the first-order and  $n^{\text{th}}$ -order probability distributions and how, in practice, the first-order probability density would be obtained from the values of the first-order moments.

The first-order probability density function  $p(x)$  and its characteristic function  $F_x(u)$  are uniquely related by the Fourier transformation:

$$F_x(u) = \int_{-\infty}^{\infty} e^{jux} p(x) dx \quad (1)$$

$$p(x) = \frac{1}{2\pi} \int_{-\infty}^{\infty} e^{-jux} F_x(u) du \quad (2)$$

Equation (1) is also the definition of the characteristic function. The characteristic function can be written in the form of a Taylor series in which the coefficients of the terms are the moments of the probability distribution.

$$F_x(u) = \sum_{n=0}^{\infty} \frac{(j u)^n}{n!} \overline{x^n} \quad (3)$$

It is clear, then, that the complete set of moments (if they exist) uniquely defines the probability density.

It is usually desirable to use only the lower-order moments (customarily, the first four moments),  $\overline{x}$ ,  $\overline{x^2}$ ,  $\overline{x^3}$ , and  $\overline{x^4}$ , to obtain the probability density. Two techniques are commonly used to provide an expansion of  $p(x)$  in terms of the moments. The earlier technique – the Gram-Charlier series and the Edgeworth expansion (7) – uses an expansion in terms of the gaussian distribution  $p_g(x)$  and its derivatives in order to approximate slightly non-gaussian distributions. Pearson's system (8) is an attempt to fit both slightly non-gaussian and markedly non-gaussian distributions by using only the first four moments. It predicates a distribution density with a single extremum and a high degree of contact with the axis for large amplitudes. It is designed for use in fitting this wide class of density functions. We have found that the Pearson system is easy to use and that it usually provides a good fit to the continuous distributions we encountered (9).

The  $n^{\text{th}}$ -order probability distribution, the  $n^{\text{th}}$ -order characteristic function, and the expansion of the  $n^{\text{th}}$ -order characteristic function in terms of the higher-order auto-correlation functions are given by extension of the first-order equations.

$$p(x_1, x_2, \dots, x_n) = \frac{1}{(2\pi)^n} \int_{-\infty}^{\infty} \dots \int_{-\infty}^{\infty} \exp\left(-i \sum_{\nu=1}^n u_{\nu} x_{\nu}\right) F_x(u_1, u_2, \dots, u_n) du_1 du_2 \dots du_n \quad (4)$$

$$F_x(u_1, u_2, \dots, u_n) = \int_{-\infty}^{\infty} \dots \int_{-\infty}^{\infty} \exp\left(i \sum_{\nu=1}^n u_{\nu} x_{\nu}\right) p(x_1, x_2, \dots, x_n) dx_1 dx_2 \dots dx_n \quad (5)$$

$$F_x(u_1, u_2, \dots, u_n) = \sum_{\nu_1=0}^{\infty} \sum_{\nu_2=0}^{\infty} \dots \sum_{\nu_n=0}^{\infty} \frac{(ju_1)^{\nu_1} (ju_2)^{\nu_2} \dots (ju_n)^{\nu_n}}{\nu_1! \nu_2! \dots \nu_n!} \overline{(x_1)^{\nu_1} (x_2)^{\nu_2} \dots (x_n)^{\nu_n}} \quad (6)$$

A higher-order Edgeworth series may be used to approximate the probability density for almost-gaussian distributions by using higher-order autocorrelation functions(10), but there is no higher-order equivalent to the Pearson system available. In this investigation attention is centered on the first-order distributions.

## 2.2 EVALUATION OF THE MOMENTS IN THE FREQUENCY DOMAIN

We now describe a technique for the evaluation of the moments and the higher-order autocorrelation functions of the output of a linear filter, in terms of the frequency response of the filter  $H(\omega)$  and the corresponding higher-order autocorrelation functions of the input variable. The relation for the moments was first stated by Mazelsky (11). We add the generalization to higher-order autocorrelation functions, together with a demonstration that as complete a characterization of the output variable as is available for the input function can be provided.

Consider an ensemble of random functions  $x(t)$  which are statistically stationary and ergodic. These functions are passed through a linear network whose impulse response is  $h(t)$  to yield the output variable  $y(t)$ .

From network theory (12), the system function of the linear system,  $H(\omega)$ , is defined as the Fourier transform of the impulse response.

$$h(t) = \frac{1}{2\pi} \int_{-\infty}^{\infty} H(\omega) e^{j\omega t} d\omega \quad (7)$$

$$H(\omega) = \int_{-\infty}^{\infty} h(t) e^{-j\omega t} dt \quad (8)$$

The relations between the input and output of the system can be written in the time domain and frequency domain as

$$y(t) = \int_{-\infty}^{\infty} h(\tau) x(t - \tau) d\tau \quad (9)$$

and

$$Y(\omega) = H(\omega) X(\omega) \quad (10)$$

where  $X(\omega)$  is the Fourier transform of  $x(t)$ , and  $Y(\omega)$  is the Fourier transform of  $y(t)$  in a sense that will be specified in Eq. (18).

The first autocorrelation function and spectral density will now be defined before we proceed to the  $n^{\text{th}}$ -order equivalents. The first-order autocorrelation function is defined (13) by the relation

$$\phi_x(\tau) = \lim_{T \rightarrow \infty} \frac{1}{2T} \int_{-T}^T x(t) x(t + \tau) dt \quad (11)$$

The Fourier transform relation defines the spectral density  $\Phi_x(\omega)$  (also called the power spectrum):

$$\Phi_x(\omega) = \int_{-\infty}^{\infty} \phi_x(\tau) e^{-j\omega\tau} d\tau \quad (12)$$

$$\phi_x(\tau) = \frac{1}{2\pi} \int_{-\infty}^{\infty} \Phi_x(\omega) e^{j\omega\tau} d\omega \quad (13)$$

By a direct extension of Eq. (11) we can define the  $n^{\text{th}}$ -order autocorrelation function as

$$\phi_x(\tau_1, \tau_2, \dots, \tau_n) = \lim_{T \rightarrow \infty} \frac{1}{2T} \int_{-T}^T x(t) x(t + \tau_1) x(t + \tau_2) \dots x(t + \tau_n) dt \quad (14)$$

The existence of this function for all values of  $\tau_1, \tau_2, \dots, \tau_n$  can be demonstrated for all time functions that would be encountered in physical measurements. The restriction to physically realizable waveforms implies that  $x(t)$  must remain finite at all times. Then all the moments of  $x(t)$  will exist. Since the maximum value of  $\phi_x(\tau_1, \tau_2, \dots, \tau_n)$  (which occurs for  $0 = \tau_1 = \tau_2 = \dots = \tau_n$ ) is the  $(n + 1)^{\text{th}}$  moment of  $x$ , then  $\phi_x(\tau_1, \tau_2, \dots, \tau_n)$  will always exist.

The corresponding  $n^{\text{th}}$ -order spectral density is defined by the multiple Fourier transform relationship:

$$\Phi_x(\omega_1, \omega_2, \dots, \omega_n) = \iint_{-\infty}^{\infty} \dots \int \phi_x(\tau_1, \tau_2, \dots, \tau_n) \exp[-j(\omega_1 \tau_1 + \omega_2 \tau_2 + \dots + \omega_n \tau_n)] d\tau_1 d\tau_2 \dots d\tau_n \quad (15)$$

$$\phi_{\mathbf{x}}(\tau_1, \tau_2, \dots, \tau_n) = \left(\frac{1}{2\pi}\right)^n \iint_{-\infty}^{\infty} \dots \int \Phi_{\mathbf{x}}(\omega_1, \omega_2, \omega_3, \dots, \omega_n) \exp[j(\omega_1\tau_1 + \omega_2\tau_2 + \dots + \omega_n\tau_n)] d\omega_1 d\omega_2 \dots d\omega_n \quad (16)$$

The  $(n + 1)^{\text{th}}$  moment of  $\mathbf{x}(t)$  can be evaluated from  $\Phi_{\mathbf{x}}(\omega_1, \omega_2, \dots, \omega_n)$ :

$$\overline{\mathbf{x}^{n+1}} = \phi_{\mathbf{x}}(0, 0, \dots, 0) = \left(\frac{1}{2\pi}\right)^n \iint_{-\infty}^{\infty} \dots \int \Phi_{\mathbf{x}}(\omega_1, \omega_2, \dots, \omega_n) d\omega_1 d\omega_2 \dots d\omega_n \quad (17)$$

This relation implies that  $\Phi_{\mathbf{x}}(\omega_1, \omega_2, \dots, \omega_n)$  is integrable and hence can have no singularities worse than delta-functions.

There is another property of the  $n^{\text{th}}$ -order spectral density which we shall establish: an expression for the spectral density in terms of the Fourier transform of the time function  $\mathbf{X}(\omega)$ . If we define the sectioned variable  $\mathbf{x}_T(t)$  as being equal to  $\mathbf{x}(t)$  in the region from  $-T$  to  $+T$  and zero elsewhere, we can write the Fourier transform of  $\mathbf{x}(t)$  as

$$\mathbf{X}_T(\omega) = \left\langle \int_{-\infty}^{\infty} \mathbf{x}_T(t) \exp(-j\omega t) dt \right\rangle \quad (18)$$

where  $\langle f(t) \rangle$  indicates the ensemble average of  $f(t)$ .

From Eq. 15, we have

$$\begin{aligned} \Phi_{\mathbf{x}}(\omega_1, \omega_2, \dots, \omega_n) &= \iint_{-\infty}^{\infty} \dots \int \left[ \lim_{T \rightarrow \infty} \frac{1}{2T} \left\langle \int_{-\infty}^{\infty} \mathbf{x}_T(t) \mathbf{x}_T(t + \tau_1) \dots \mathbf{x}_T(t + \tau_n) dt \right\rangle \right] \\ &\quad \times \exp[-j(\omega_1\tau_1 + \omega_2\tau_2 + \dots + \omega_n\tau_n)] d\tau_1 d\tau_2 \dots d\tau_n \\ &= \lim_{T \rightarrow \infty} \frac{1}{2T} \left\langle \left[ \int_{-\infty}^{\infty} \mathbf{x}_T(t + \tau_1) \exp[-j\omega_1(t + \tau_1)] d\tau_1 \right] \left[ \int_{-\infty}^{\infty} \mathbf{x}_T(t + \tau_2) \exp[-j\omega_2(t + \tau_2)] d\tau_2 \right] \right. \\ &\quad \left. \dots \left[ \int_{-\infty}^{\infty} \mathbf{x}_T(t + \tau_n) \exp[-j\omega_n(t + \tau_n)] d\tau_n \right] \left[ \int_{-\infty}^{\infty} \mathbf{x}_T(t) \exp[j(\omega_1 + \omega_2 + \dots + \omega_n)t] dt \right] \right\rangle \end{aligned}$$

Therefore,

$$\Phi_{\mathbf{x}}(\omega_1, \omega_2, \dots, \omega_n) = \lim_{T \rightarrow \infty} \frac{1}{2T} \mathbf{X}_T(\omega_1) \mathbf{X}_T(\omega_2) \dots \mathbf{X}_T(\omega_n) \mathbf{X}_T^*(\omega_1 + \omega_2 + \dots + \omega_n) \quad (19)$$

which, in general, contains delta-functions, but is integrable in  $\omega$ -space.

Next we evaluate the  $(n + 1)^{\text{th}}$ -order moment of  $\mathbf{y}(t)$ :

$$\overline{\mathbf{y}^{n+1}} = \lim_{T \rightarrow \infty} \frac{1}{2T} \int_{-T}^T [\mathbf{y}(t)]^{n+1} dt \quad (20)$$

We can substitute for  $y(t)$  from the convolution equation (Eq. (9)).

$$\begin{aligned}
\overline{y^{n+1}} &= \lim_{T \rightarrow \infty} \frac{1}{2T} \int_{-T}^T \left[ \int_{-\infty}^{\infty} h(\sigma_1) x(t - \sigma_1) d\sigma_1 \right] \left[ \int_{-\infty}^{\infty} h(\sigma_2) x(t - \sigma_2) d\sigma_2 \right] \dots \left[ \int_{-\infty}^{\infty} h(\sigma_{n+1}) x(t - \sigma_{n+1}) d\sigma_{n+1} \right] dt \\
&= \iint_{-\infty}^{\infty} \dots \int h(\sigma_1) h(\sigma_2) \dots h(\sigma_{n+1}) d\sigma_1 d\sigma_2 \dots d\sigma_{n+1} \\
&\quad \times \lim_{T \rightarrow \infty} \frac{1}{2T} \int_{-T}^T x(t - \sigma_1) x(t - \sigma_2) \dots x(t - \sigma_{n+1}) dt \\
&= \iint_{-\infty}^{\infty} \dots \int h(\sigma_1) h(\sigma_2) \dots h(\sigma_{n+1}) \phi_x(\sigma_1 - \sigma_2, \sigma_1 - \sigma_3, \dots, \sigma_1 - \sigma_{n+1}) d\sigma_1 d\sigma_2 \dots d\sigma_{n+1} \\
&= \iint_{-\infty}^{\infty} \dots \int h(\sigma_1) h(\sigma_2) \dots h(\sigma_{n+1}) \left[ \left( \frac{1}{2\pi} \right)^n \iint_{-\infty}^{\infty} \dots \int \Phi_x(\omega_1, \omega_2, \dots, \omega_n) \right. \\
&\quad \left. \times \exp \{j[\omega_1(\sigma_1 - \sigma_2) + \omega_2(\sigma_1 - \sigma_3) + \dots + \omega_n(\sigma_1 - \sigma_{n+1})]\} d\omega_1 d\omega_2 \dots d\omega_n \right] d\sigma_1 d\sigma_2 \dots d\sigma_{n+1} \\
\overline{y^{n+1}} &= \left( \frac{1}{2\pi} \right)^n \iint_{-\infty}^{\infty} \dots \int \Phi_x(\omega_1, \omega_2, \dots, \omega_n) H(\omega_1) H(\omega_2) \dots H(\omega_n) \\
&\quad \times H^*(\omega_1 + \omega_2 + \dots + \omega_n) d\omega_1 d\omega_2 \dots d\omega_n
\end{aligned} \tag{21}$$

In the light of Eqs. (19) and (10), this relation indicates that we could have written more simply:

$$\begin{aligned}
\overline{y^{n+1}} &= \left( \frac{1}{2\pi} \right)^n \iint_{-\infty}^{\infty} \dots \int \lim_{T \rightarrow \infty} \frac{1}{2T} Y_T(\omega_1) Y_T(\omega_2) \dots Y_T(\omega_n) Y_T^*(\omega_1 + \omega_2 + \dots + \omega_n) \\
&\quad \times d\omega_1 d\omega_2 \dots d\omega_n \\
&= \left( \frac{1}{2\pi} \right)^n \iint_{-\infty}^{\infty} \dots \int \lim_{T \rightarrow \infty} \frac{1}{2T} [X_T(\omega_1) X_T(\omega_2) \dots X_T(\omega_n) X_T^*(\omega_1 + \omega_2 + \dots + \omega_n)] \\
&\quad \times [H(\omega_1) H(\omega_2) \dots H(\omega_n) H^*(\omega_1 + \omega_2 + \dots + \omega_n)] d\omega_1 d\omega_2 \dots d\omega_n
\end{aligned}$$

which yields the same result. It is clear that in general the  $n^{\text{th}}$ -order spectral densities of the input and output of a linear system are related by

$$\Phi_y(\omega_1, \omega_2, \dots, \omega_n) = \Phi_x(\omega_1, \omega_2, \dots, \omega_n) H(\omega_1) H(\omega_2) \dots H(\omega_n) H^*(\omega_1 + \omega_2 + \dots + \omega_n) \tag{22}$$

The existence of this relationship means that given the  $n^{\text{th}}$ -order autocorrelation function or the  $n^{\text{th}}$ -order spectral density of an arbitrary random function which is the input to a linear filter, we can obtain that autocorrelation function or spectral density of the output which is of the same order. This technique, then, provides as much

information about the output of the linear system as we know about the input. Our attention, it should be emphasized, is fixed on the autocorrelation functions and the power spectra rather than on the probability densities. This is permissible, since the probability densities are uniquely defined by the autocorrelation functions.

It must be noted that the application of these techniques to any actual problem is quite complicated and that, in general, machine computation would be required. The characterization of a distribution may be quite approximate, however. Frequently, one is interested only in the first-order probability density or the first- and second-order distributions. For these limited goals, the moments technique is useful.

### 2.3 EVALUATION OF THE MOMENTS IN THE TIME DOMAIN FOR RANDOM-PULSE NOISE

For the class of random functions that consist of the sum of a series of pulses whose initiation times are randomly distributed, Middleton's simple and direct technique (14) enables us to obtain the moments in the time domain. We shall use this technique to examine the effect of linear systems on the moments only, but the higher-order autocorrelation functions can also be obtained from Middleton's equations.

The proof of the Middleton relations presented here is simpler than that provided by Middleton (15) because we are interested only in the first-order characteristic function.

Consider a function  $x_K(t)$  which consists of the sum of  $K$  randomly occurring pulses in an interval  $(0, T)$ , and for which  $K$  itself is a random variable with a Poisson distribution. Then we can write

$$x_K(t) = \sum_{k=1}^K a_k e(t - t_k ; r_k) \quad (23)$$

where  $a_k$  is the amplitude coefficient of the  $k^{\text{th}}$  pulse,  $r_k$  is a duration coefficient for the  $k^{\text{th}}$  pulse, and  $t_k$  is the occurrence time of the  $k^{\text{th}}$  pulse.  $K$ ,  $a_k$ ,  $r_k$ , and  $t_k$  are independent random variables for which the probability density functions are  $p_1(K)$ ,  $p_2(a_k)$ ,  $p_3(r_k)$ , and  $p_4(t_k)$ , respectively. The characteristic function of a single pulse can be written:

$$F_{x_1}(u) = \int_{-\infty}^{\infty} \int_0^{\infty} \int_0^T \exp [ju a_k e(t - t_k ; r_k)] p_2(a_k) p_3(r_k) p_4(t_k) da_k dr_k dt_k \quad (24)$$

Since the pulses are independent of each other, the characteristic function of the random variable  $x(t)$  can be obtained, using the Poisson nature of  $p_1(K)$ , as

$$\begin{aligned}
F_x(u) &= \sum_{K=0}^{\infty} p_1(K) \left[ \prod_{k=1}^K F_{x_1}(u) \right]^* \\
&= \sum_{K=0}^{\infty} \frac{(\bar{N}T)^K}{K!} \exp(-\bar{N}T) [F_{x_1}(u)]^K \\
&= \exp[-\bar{N}T + \bar{N}T F_{x_1}(u)]
\end{aligned}$$

where  $\bar{N}$  is the average number of pulses per second.

$$\begin{aligned}
F_x(u) &= \exp \left\{ -\bar{N}T + \bar{N}T \int_{-\infty}^{\infty} \int_0^{\infty} \int_0^T \exp [ju a_k e(t - t_k ; r_k)] p_2(a_k) p_3(r_k) p_4(t_k) da_k dr_k dt_k \right\} \\
&= \exp \left\{ \bar{N}T \int_{-\infty}^{\infty} \int_0^{\infty} \int_0^T \left[ \exp [ju a_k e(t - t_k ; r_k)] - 1 \right] p_2(a_k) p_3(r_k) p_4(t_k) da_k dr_k dt_k \right\}
\end{aligned}$$

The assumption of a random pulse initiation time in the interval  $(0, T)$  means that  $p_4(t_k) = 1/T$  for  $0 < t_k < T$  and zero elsewhere. If we assume that the duration of the pulses is short compared with  $T$ , we can extend the upper limit of integration for  $t_k$  to infinity. Let us further assume that the pulse parameter distributions are the same for all pulses.

Then

$$F_x(u) = \exp \left\{ \bar{N} \int_{-\infty}^{\infty} \int_0^{\infty} \int_0^{\infty} \left[ \exp [ju a e(t - t_k ; r)] - 1 \right] p_2(a) p_3(r) da dr dt_k \right\}$$

Since the process is assumed to be stationary, we can set  $t = 0$ . We also substitute  $\rho = -t_k$  to obtain the final form:

$$F_x(u) = \exp \left\{ \bar{N} \int_{-\infty}^{\infty} \int_0^{\infty} \int_0^{\infty} \left[ \exp [ju a e(\rho ; r)] - 1 \right] p_2(a) p_3(r) da dr d\rho \right\} \quad (25)$$

Let us apply this expression to the particular case in which  $p_2(a) = \delta(a - a_0)$ ,  $p_3(r) = \delta(r - r_0)$ ,  $e(\rho, r) = 1$ , for  $0 < \rho < r$  and zero elsewhere. Therefore,

$$\begin{aligned}
F_x(u) &= \exp \left\{ \bar{N} \int_0^{r_0} \left[ \exp(ju a_0) - 1 \right] d\rho \right\} \\
&= \exp [\bar{N} r_0 (\exp(ju a_0) - 1)]
\end{aligned} \quad (26)$$

This is the characteristic function for a Poisson distribution (16); therefore, we can write

$$p\left(\frac{x}{a_0}\right) = \frac{[\bar{N} r_0]^{x/a_0}}{\left(\frac{x}{a_0}\right)!} \exp(-\bar{N} r_0) \delta\left(\frac{x}{a_0} - n\right) \quad n = 0, 1, 2, \dots \quad (27)$$



Usually, the evaluation of  $F_x(u)$  in closed form and the subsequent Fourier transformation are not feasible. In such cases, it is usually possible to obtain the semi-invariants and moments.

The semi-invariants or cumulants are defined (17) by the equation

$$F_x(u) = \exp \left[ \sum_{m=1}^{\infty} K_m \frac{(ju)^m}{m!} \right] \quad (28)$$

We can put Eq. (25) into this form by using the series expansion for the exponential function, which yields

$$\begin{aligned} F_x(u) &= \exp \left\{ \bar{N} \int_{-\infty}^{\infty} \int_0^{\infty} \int_0^{\infty} \sum_{m=1}^{\infty} \frac{[juae(\rho; r)]^m}{m!} p_2(a) p_3(r) da dr d\rho \right\} \\ &= \exp \left\{ \sum_{m=1}^{\infty} \frac{(ju)^m}{m!} \left[ \bar{N} \int_{-\infty}^{\infty} \int_0^{\infty} \int_0^{\infty} a^m e^{m(\rho; r)} p_2(a) p_3(r) da dr d\rho \right] \right\} \end{aligned} \quad (29)$$

Therefore,

$$K_m = \bar{N} \int_{-\infty}^{\infty} \int_0^{\infty} \int_0^{\infty} a^m e^{m(\rho; r)} p_2(a) p_3(r) da dr d\rho \quad (30)$$

This expression can usually be evaluated, and the  $n^{\text{th}}$ -order moment can then be obtained from the  $n^{\text{th}}$ -order semi-invariant (17).

The use of this time-domain technique permits us to examine the effects of various network configurations and parameters on a type of non-gaussian noise that appears frequently in models of noise processes. The effects of a variety of networks are examined in the appendix.

### III. SOME APPLICATIONS OF THE MOMENTS TECHNIQUE

The relations established in Section II for the moments in the time domain and frequency domain will now be applied. The frequency-domain techniques will be used in examining the nature of the approach to a gaussian distribution for random-pulse noise which is sharply band-limited as the bandwidth goes to zero. Section 3.1 is devoted to establishing the nature of the higher-order autocorrelation functions and spectral densities. The effects of band-limiting will be considered in section 3.2. In section 3.3 we shall consider the effect on the distribution of eliminating the low-frequency energy in random-pulse noise, and illustrate the application of the moments technique in the time domain.

#### 3.1 EVALUATION OF THE HIGHER-ORDER POWER SPECTRA FOR RANDOM-PULSE NOISE

The complete expressions for the first-, second-, and third-order spectral densities of random-pulse noise will now be presented, and the nature of the terms in the general  $n^{\text{th}}$ -order spectral density will be discussed. It should be pointed out that this is actually the same random variable that was treated in section 2.3, the initial assumption made here, that all the pulses are identical, being removed by a suitable averaging technique later in the development.

We consider a random function of time  $x(t)$  which is the sum of a series of randomly occurring pulses, all of which have the same waveform. The sectioned function exists only in the interval  $(-T, T)$ , where  $T$  is very much greater than the individual pulse length, and can be written

$$x_T(t) = \sum_{n=1}^N f(t - t_n) \quad (31)$$

where  $t_n$  is a random variable with a uniform distribution in the interval  $(-T, +T)$ . The average pulse density is  $\bar{N} = \langle N/2T \rangle$ . Since the individual pulses exist only for a length of time small compared with  $T$ , the usual autocorrelation function of an individual pulse goes to zero in the limit as  $T \rightarrow \infty$ . In this section, therefore, we shall use a modified  $n^{\text{th}}$ -order autocorrelation function,  $\tilde{\phi}_f(\tau_1, \tau_2, \dots, \tau_n)$ , for the individual pulse, which is defined by:

$$\tilde{\phi}_f(\tau_1, \tau_2, \dots, \tau_n) = \int_{-\infty}^{\infty} f(t) f(t + \tau_1) \dots f(t + \tau_n) dt \quad (32)$$

The modified spectral density is defined as the Fourier transform of  $\tilde{\phi}_f(\tau_1, \tau_2, \dots, \tau_n)$ . It can then be shown that

$$\tilde{\Phi}_f(\omega_1, \omega_2, \dots, \omega_n) = F(\omega_1) F(\omega_2) \dots F(\omega_n) F^*(\omega_1 + \omega_2 + \dots + \omega_n) \quad (33)$$

where

$$F(\omega) = \int_{-\infty}^{\infty} f(t) \exp(-j\omega t) dt \quad (34)$$

Instead of the mean value of  $f(t)$ , we shall use

$$\bar{f} = \int_{-\infty}^{\infty} f(t) dt = F(0)$$

We shall now examine the first-order autocorrelation function of  $x(t)$ .

$$\phi_x(\tau) = \lim_{T \rightarrow \infty} \frac{1}{2T} \int_{-T}^T \left[ \sum_{m=1}^N f(t - t_m) \right] \left[ \sum_{n=1}^N f(t - t_n + \tau) \right] dt \quad (35)$$

We distinguish two separate cases here: where  $n = m$  and where it does not.

$$\phi_x(\tau) = \lim_{T \rightarrow \infty} \frac{1}{2T} \int_{-T}^T \left[ \sum_{m=1}^N f(t - t_m) f(t - t_m + \tau) + \sum_{\substack{m=1 \\ m \neq n}}^N \sum_{n=1}^N f(t - t_m) f(t - t_n + \tau) \right] dt \quad (36)$$

The first term is merely the modified autocorrelation function of an individual pulse and thus it yields

$$\lim_{T \rightarrow \infty} \frac{1}{2T} N \tilde{\phi}_f(\tau) = \bar{N} \tilde{\phi}_f(\tau) \quad (37)$$

In evaluating the second term we recall that the initiation times are independent random variables with probability density  $1/2T$  in the interval  $(-T, +T)$  and zero elsewhere. The contribution from this term must be a constant, since, on an ensemble basis, the probability of overlap of the pulses  $f(t - t_a)$  and  $f(t - t_b + \tau)$  is independent of  $\tau$ . If the displacement between the initiation times of the two pulses,  $t_a - t_b + \tau$ , lies in the interval  $(t_d, t_d + dt_d)$ , then the contribution from this term will be

$$\tilde{\phi}_f(t_d) = \int_{-\infty}^{\infty} f(t) f(t + t_d) dt \quad (38)$$

The probability that the displacement time will be within this interval is  $dt_d/2T$ . There are  $N(N-1)$  such contributions in the second term. Therefore, the value of the second term is

$$\begin{aligned} \lim_{T \rightarrow \infty} \frac{1}{2T} \left[ N(N-1) \int_{-T}^T \tilde{\phi}_f(t_d) \frac{dt_d}{2T} \right] &= \lim_{T \rightarrow \infty} \frac{N(N-1)}{(2T)^2} \tilde{\phi}_f(0) \\ &= \lim_{T \rightarrow \infty} \frac{N(N-1)}{(2T)^2} \tilde{f}^2 = \bar{N}^2 \tilde{f}^2 \end{aligned} \quad (39)$$

We can see this result more directly by noting that the first term contains all of the contributions from pulses overlapping with themselves, while the second term contains all of the contributions from random overlapping with the other pulses. For

two statistically independent random variables, the mean of their product is the product of their means: The mean of each variable is  $\bar{N} \tilde{f}$ ; therefore, the contribution from the second term should be  $\bar{N}^2 \tilde{f}^2$ . Both of these trains of logic will be employed freely in the development of the higher-order autocorrelation functions.

The expression for the autocorrelation function of a sum of identical randomly-occurring pulses of density  $\bar{N}$  pulses per second thus becomes

$$\phi_x(\tau) = \bar{N} \tilde{\phi}_f(\tau) + \bar{N}^2 \tilde{f}^2 \quad (40)$$

Fourier transformation of this result yields the first-order spectral density

$$\Phi_x(\omega) = \bar{N} \tilde{\Phi}_f(\omega) + 2\pi \bar{N}^2 \tilde{f}^2 \delta(\omega) \quad (41)$$

Next, we consider the second-order autocorrelation function.

$$\phi_x(\tau_1, \tau_2) = \lim_{T \rightarrow \infty} \frac{1}{2T} \int_{-T}^T \left[ \sum_{\ell=1}^N f(t - t_\ell) \right] \left[ \sum_{m=1}^N f(t - t_m + \tau_1) \right] \left[ \sum_{n=1}^N f(t - t_n + \tau_2) \right] dt \quad (42)$$

Three cases can be distinguished here: all of the indices are identical; one index differs from the other two; all three indices differ.

When all of the indices are identical:

$$\begin{aligned} \lim_{T \rightarrow \infty} \frac{1}{2T} \int_{-T}^T \left[ \sum_{\ell=1}^N f(t - t_\ell) f(t - t_\ell + \tau_1) f(t - t_\ell + \tau_2) \right] dt &= \lim_{T \rightarrow \infty} \frac{1}{2T} \sum_{\ell=1}^N \tilde{\phi}_{f\ell}(\tau_1, \tau_2) \\ &= \bar{N} \tilde{\phi}_f(\tau_1, \tau_2) \end{aligned}$$

If one index differs from the other two, we get three possible terms:

$$\begin{aligned} \lim_{T \rightarrow \infty} \frac{1}{2T} \int_{-T}^T \sum_{\substack{\ell=1 \\ \ell \neq m}}^N \sum_{m=1}^N [f(t - t_\ell) f(t - t_\ell + \tau_1) f(t - t_m + \tau_2) + f(t - t_\ell) f(t - t_m + \tau_1) f(t - t_\ell + \tau_2) \\ + f(t - t_m) f(t - t_\ell + \tau_1) f(t - t_\ell + \tau_2)] dt \end{aligned}$$

We consider the first of these terms and then generalize the result, thus obtaining a complete expression for the case in which one index differs from the other two.

$$\lim_{T \rightarrow \infty} \frac{1}{2T} \int_{-T}^T \sum_{\substack{\ell=1 \\ \ell \neq m}}^N \sum_{m=1}^N [f(t - t_\ell) f(t - t_\ell + \tau_1) f(t - t_m + \tau_2)] dt$$

We notice first that the values of these terms must be constant with respect to  $\tau_2$ , since  $t_\ell$  and  $t_m$  are independent random variables. If we define  $f(t - t_\ell) f(t - t_\ell + \tau_1)$  as a new variable  $g(t - t_\ell)$ , we can apply the same reasoning that we used for the second part of the first-order autocorrelation function, and thus obtain

$$\begin{aligned}
& \lim_{T \rightarrow \infty} \frac{1}{2T} \left[ N(N-1) \int_{-T}^T \int_{-T}^T g(t-t_\ell) f(t-t_\ell+t_d) dt \frac{dt_d}{T} \right] \\
&= \lim_{T \rightarrow \infty} \frac{1}{2T} \left[ N(N-1) \tilde{f} \int_{-T}^T f(t-t_\ell) f(t-t_\ell+\tau_1) dt \right] \\
&= \bar{N}^2 \tilde{\phi}_f(\tau_1) \tilde{f}
\end{aligned}$$

Therefore

$$\lim_{T \rightarrow \infty} \frac{1}{2T} \int_{-T}^T \sum_{\ell=1}^N \sum_{\substack{m=1 \\ \ell \neq m}}^N [f(t-t_\ell) f(t-t_\ell+\tau_1) f(t-t_m+\tau_2)] dt = \bar{N}^2 \tilde{f} \tilde{\phi}_f(\tau_1)$$

Generalizing from this result, we see that the terms in which one index differs from the other two are equal to

$$\bar{N}^2 \tilde{f} [\tilde{\phi}_f(\tau_1) + \tilde{\phi}_f(\tau_2) + \tilde{\phi}_f(\tau_1 - \tau_2)]$$

The case in which all three indices are different requires application of the same techniques. We have

$$\lim_{T \rightarrow \infty} \frac{1}{2T} \int_{-T}^T \sum_{\substack{\ell=1 \\ \ell \neq m \neq n \neq \ell}}^N \sum_{m=1}^N \sum_{n=1}^N f(t-t_\ell) f(t-t_m+\tau_1) f(t-t_n+\tau_2) dt$$

The result will be a constant, since  $t_\ell$ ,  $t_m$ , and  $t_n$  are independent random variables. Consider the situation in which  $t_\ell - t_m + \tau_1$  lies in the interval  $(t_{d1}, t_{d1} + dt_{d1})$  and  $t_\ell - t_n + \tau_2$  lies in the interval  $(t_{d2}, t_{d2} + dt_{d2})$  for  $t_{d1}$  and  $t_{d2}$  within the interval  $(-T, T)$ . The probability of this situation arising is  $\frac{dt_{d1} dt_{d2}}{(2T)^2}$ . The value of the

integral of the product at this point is  $\tilde{\phi}_f(t_{d1}, t_{d2})$ . There are  $N(N-1)(N-2)$  possible ways in which this can occur. Therefore, for the third case, we find:

$$\begin{aligned}
\lim_{T \rightarrow \infty} \frac{1}{2T} N(N-1)(N-2) \int_{-T}^T \int_{-T}^T \tilde{\phi}_f(t_{d1}, t_{d2}) \frac{dt_{d1}}{2T} \frac{dt_{d2}}{2T} &= \bar{N}^3 \tilde{\phi}_f(0,0) \\
&= \bar{N}^3 \tilde{f}^3
\end{aligned}$$

Therefore, the second-order autocorrelation function can be written:

$$\phi_x(\tau_1, \tau_2) = \bar{N} \tilde{\phi}_f(\tau_1, \tau_2) + \bar{N}^2 \tilde{f} [\tilde{\phi}_f(\tau_1) + \tilde{\phi}_f(\tau_2) + \tilde{\phi}_f(\tau_1 - \tau_2)] + \bar{N}^3 \tilde{f}^3 \quad (43)$$

The second-order spectral density is evaluated by a Fourier transformation:

$$\begin{aligned}
\Phi_x(\omega_1, \omega_2) &= \bar{N} \tilde{\Phi}_f(\omega_1, \omega_2) + 2\pi \bar{N}^2 \tilde{f} [\tilde{\Phi}_f(\omega_1) \delta(\omega_2) + \tilde{\Phi}_f(\omega_2) \delta(\omega_1) + \tilde{\Phi}_f(\omega_1) \delta(\omega_1 + \omega_2)] \\
&\quad + (2\pi)^2 \bar{N}^3 \tilde{f}^3 \delta(\omega_1) \delta(\omega_2)
\end{aligned} \quad (44)$$

The third-order autocorrelation function can be found by an extension of these methods.

$$\begin{aligned} \phi_x(\tau_1, \tau_2, \tau_3) = & \lim_{T \rightarrow \infty} \frac{1}{2T} \int_{-T}^T \left[ \sum_{k=1}^N f(t - t_k) \right] \left[ \sum_{\ell=1}^N f(t - t_\ell + \tau_1) \right] \\ & \times \left[ \sum_{m=1}^N f(t - t_m + \tau_2) \right] \left[ \sum_{n=1}^N f(t - t_n + \tau_3) \right] dt \end{aligned} \quad (45)$$

Here we can distinguish five cases: (1) all of the indices are identical, (2) three of the indices are identical and one differs, (3) the indices are identical in two pairs which differ from each other, (4) two indices are identical but the other two differ from this pair and from each other, and (5) all of the indices differ. Now we can obtain the correlation function by the same procedure that was used earlier, and we find (listing the results for the five cases in the proper order) that:

$$\begin{aligned} \phi_x(\tau_1, \tau_2, \tau_3) = & \bar{N} \tilde{\phi}_f(\tau_1, \tau_2, \tau_3) \\ & + \bar{N}^2 \tilde{f} [\tilde{\phi}_f(\tau_1, \tau_2) + \tilde{\phi}_f(\tau_1, \tau_3) + \tilde{\phi}_f(\tau_2, \tau_3) + \tilde{\phi}_f(\tau_2 - \tau_1, \tau_3 - \tau_1)] \\ & + \bar{N}^2 [\tilde{\phi}_f(\tau_1) \tilde{\phi}_f(\tau_3 - \tau_2) + \tilde{\phi}_f(\tau_2) \tilde{\phi}_f(\tau_3 - \tau_1) + \tilde{\phi}_f(\tau_3) \tilde{\phi}_f(\tau_2 - \tau_1)] \\ & + \bar{N}^3 \tilde{f}^2 [\tilde{\phi}_f(\tau_1) + \tilde{\phi}_f(\tau_2) + \tilde{\phi}_f(\tau_3) + \tilde{\phi}_f(\tau_3 - \tau_2) + \tilde{\phi}_f(\tau_3 - \tau_1) + \tilde{\phi}_f(\tau_2 - \tau_1)] \\ & + \bar{N}^4 \tilde{f}^4 \end{aligned} \quad (46)$$

The usual Fourier transformation leads to the corresponding third-order spectral density.

$$\begin{aligned} \Phi_x(\omega_1, \omega_2, \omega_3) = & \bar{N} \tilde{\Phi}_f(\omega_1, \omega_2, \omega_3) \\ & + 2\pi \bar{N}^2 \tilde{f} [\tilde{\Phi}_f(\omega_1, \omega_2) \delta(\omega_3) + \tilde{\Phi}_f(\omega_1, \omega_3) \delta(\omega_2) + \tilde{\Phi}_f(\omega_2, \omega_3) \delta(\omega_1) \\ & \quad + \tilde{\Phi}_f(\omega_2, \omega_3) \delta(\omega_1 + \omega_2 + \omega_3)] \\ & + 2\pi \bar{N}^2 [\tilde{\Phi}_f(\omega_1) \tilde{\Phi}_f(\omega_3) \delta(\omega_2 + \omega_3) + \tilde{\Phi}_f(\omega_2) \tilde{\Phi}_f(\omega_3) \delta(\omega_1 + \omega_3) \\ & \quad + \tilde{\Phi}_f(\omega_3) \tilde{\Phi}_f(\omega_2) \delta(\omega_1 + \omega_2)] \\ & + (2\pi)^2 \bar{N}^3 \tilde{f}^2 [\tilde{\Phi}_f(\omega_1) \delta(\omega_2) \delta(\omega_3) + \tilde{\Phi}_f(\omega_2) \delta(\omega_1) \delta(\omega_3) + \tilde{\Phi}_f(\omega_3) \delta(\omega_1) \delta(\omega_2) \\ & \quad + \tilde{\Phi}_f(\omega_3) \delta(\omega_1) \delta(\omega_2 + \omega_3) + \tilde{\Phi}_f(\omega_3) \delta(\omega_2) \delta(\omega_1 + \omega_3) \\ & \quad + \tilde{\Phi}_f(\omega_2) \delta(\omega_3) \delta(\omega_1 + \omega_2)] \\ & + (2\pi)^3 \bar{N}^4 \tilde{f}^4 \delta(\omega_1) \delta(\omega_2) \delta(\omega_3) \end{aligned} \quad (47)$$

The generalization of this technique to  $n^{\text{th}}$ -order autocorrelation functions and spectral densities is rather lengthy, but possible. It is usually sufficient, however, merely to note the nature of the various terms of which these functions consist.

We first consider the  $n^{\text{th}}$ -order autocorrelation function. We must consider  $n + 1$  indices. Let us take the case in which the indices are equal in groups of  $m_1, m_2, \dots, m_a$  so that  $m_1 + m_2 + \dots + m_a = n + 1$ . The spectral-density terms that correspond to this situation will be of the form

$$\begin{aligned} & [\tilde{\Phi}_f(\omega_1, \omega_2, \dots, \omega_{m_1-1})] \times [\tilde{\Phi}_f(\omega_{m_1}, \omega_{m_1+1}, \dots, \omega_{m_1+m_2-1}) \delta(\omega_{m_1} + \omega_{m_1+1} + \dots + \omega_{m_1+m_2})] \times \dots \\ & \times [\tilde{\Phi}_f(\omega_{m_1+m_2+\dots+m_{a-1}}, \omega_{m_1+m_2+\dots+m_{a-1}+1}, \dots, \omega_{n-1})] \\ & \times \delta(\omega_{m_1+m_2+\dots+m_{a-1}} + \omega_{m_1+m_2+\dots+m_{a-1}+1} + \dots + \omega_{n-1} + \omega_n) \end{aligned} \quad (48)$$

This general expression will be of considerable use in section 3.2 in which we examine the nature of the approach to gaussian statistics when this type of noise is band-limited.

We have now developed the first-, second-, and third-order autocorrelation functions and power spectra for a function that is the sum of identical random pulses of density  $\bar{N}$  pulses per second. In addition, we have examined the general characteristics of terms in the  $n^{\text{th}}$ -order spectral density.

The extension of these results to the case in which the pulses are not identical but are determined by the values of some parameters,  $\beta_1, \beta_2, \dots, \beta_b$ , whose joint probability distribution,  $p(\beta_1, \beta_2, \dots, \beta_b)$ , is known, can be found by use of the relation

$$\tilde{\Phi}_f(\tau_1, \tau_2, \dots, \tau_n) = \iint_{-\infty}^{\infty} \dots \int \tilde{\Phi}_f_{\beta_1, \beta_2, \dots, \beta_b}(\tau_1, \tau_2, \dots, \tau_n) p(\beta_1, \beta_2, \dots, \beta_b) d\beta_1, d\beta_2, \dots, d\beta_b$$

since the pulses are still independent of each other.

### 3.2 THE APPROACH TO A GAUSSIAN DISTRIBUTION OF FILTERED RANDOM-PULSE NOISE: AN APPLICATION OF THE MOMENTS TECHNIQUE IN THE FREQUENCY DOMAIN

We can now present a proof of the approach to a gaussian distribution of random-pulse noise when it is passed through a narrow-band filter with abrupt cutoff limits. While the usual proof by the Central Limit Theorem (18) is applicable to this type of noise, the proof by the moments technique provides additional information about the nature of the approach to a gaussian distribution – and especially about the way the odd moments vanish as the bandwidth is reduced. This proof provides an example of the application of the moments method in the frequency domain. Other examples of applications of this technique are given in reference 9. We shall consider the first four moments in detail to illustrate the technique and then discuss the nature of the approach to a gaussian distribution of the higher-order moments.

Let us consider an idealized bandpass network for which  $H(\omega)$  has the form shown in Fig. 1. Since no dc is passed by this network [ $H(0) = 0$ ] it is clear that the mean of the output distribution will be zero.

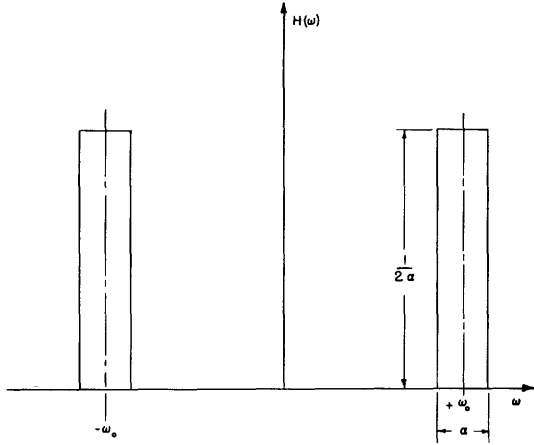


Fig. 1. The system function,  $H(\omega)$ , for an idealized bandpass network.

The first-order spectral density of random-pulse noise is given in Eq. 41. From Eq. 16,

$$\begin{aligned}\Phi_y(\omega) &= H(\omega) H^*(\omega) \Phi_x(\omega) \\ &= H(\omega) H^*(\omega) [\bar{N} \tilde{\Phi}_f(\omega) + 2\pi \bar{N}^2 \tilde{f}^2 \delta(\omega)]\end{aligned}\quad (49)$$

Since the network passes no dc, the second term gives zero contribution. We assume that  $\tilde{\Phi}_f(\omega)$  is a smooth function within the pass region of the filter and that it can be approximated by  $\tilde{\Phi}_f(\omega_0)$  throughout this region. This is not a necessary condition for the application of the moments technique but, by simplifying

the algebra, it allows us to focus our attention on the effects of the network on the moments. (This same technique will be used for the higher-order spectral densities.) Making this assumption, we get

$$\Phi_y(\omega) = \begin{cases} \frac{\bar{N} \tilde{\Phi}_f(\omega_0)}{(2a)^2} & \omega_0 - \frac{a}{2} < |\omega| < \omega_0 + \frac{a}{2} \\ 0 & \text{elsewhere} \end{cases}\quad (50)$$

From which we obtain

$$\overline{y^2} = \frac{1}{2\pi} \int_{-\infty}^{\infty} \Phi_y(\omega) d\omega = \frac{1}{2\pi} \frac{\bar{N} \tilde{\Phi}_f(\omega_0)}{2a}\quad (51)$$

If we examine the second-order spectral density in Eq. (44), we see that we can immediately eliminate most of the terms. All terms which include the function  $\delta(\omega_1)$ ,  $\delta(\omega_2)$ , or  $\delta(\omega_1 + \omega_2)$  give zero contribution to the third moment of  $y(t)$ , since  $H(\omega_1)$ ,  $H(\omega_2)$ , and  $H^*(\omega_1 + \omega_2)$  are involved in the evaluation of  $\overline{y^3}$ . The one remaining term is  $\bar{N} \tilde{\Phi}_f(\omega_1, \omega_2)$ .

Therefore,

$$\Phi_y(\omega_1, \omega_2) = \bar{N} \tilde{\Phi}_f(\omega_1, \omega_2) H(\omega_1) H(\omega_2) H^*(\omega_1 + \omega_2)\quad (52)$$

Since  $\overline{y^3}$  equals the integral of this function in the  $\omega_1, \omega_2$  plane, let us examine the regions in this plane for which the function is nonzero. In Fig. 2a we consider the narrow-band case in which  $\alpha < 2/3 \omega_0$  and in Fig. 2b we consider the situation in which  $\alpha > 2/3 \omega_0$ . It can be seen from Fig. 2a that there are no regions in which the product  $H(\omega_1) H(\omega_2) H^*(\omega_1 + \omega_2)$  is nonzero. The third moment is always zero for  $\alpha < 2/3 \omega_0$ . From Fig. 2b it can be seen that the total area of the region of overlap is

$$\frac{3}{4} (3a - 2\omega_0)^2 = \frac{27}{4} \left(a - \frac{2}{3} \omega_0\right)^2$$



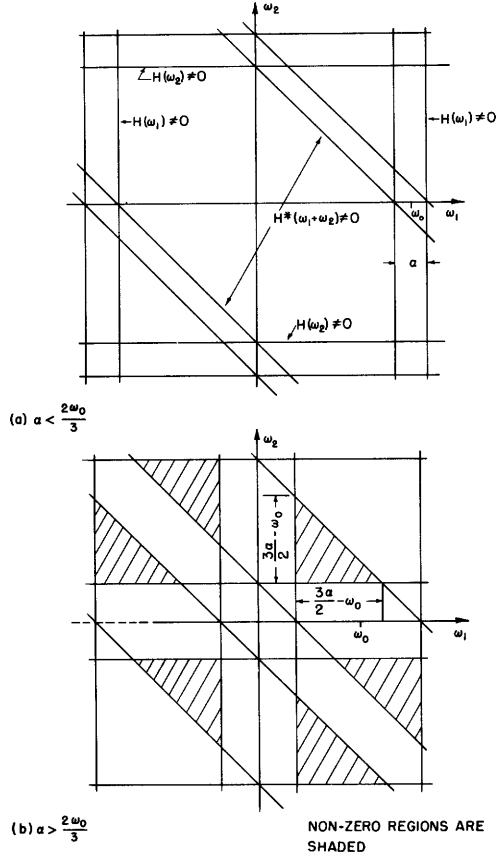


Fig. 2. Nonzero regions in the  $\omega_1 - \omega_2$  plane for the function  $H(\omega_1) \cdot H(\omega_2) \cdot H^*(\omega_1 + \omega_2)$ .

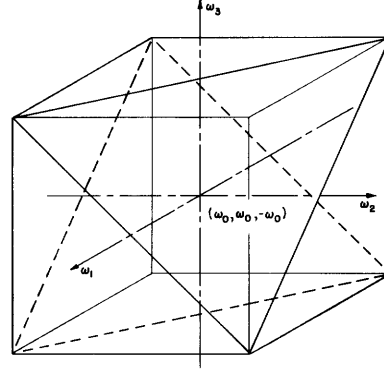


Fig. 3. The volume centered at  $(\omega_0, \omega_0, -\omega_0)$  in which the function  $H(\omega_1) \cdot H(\omega_2) \cdot H(\omega_3) \cdot H^*(\omega_1 + \omega_2 + \omega_3)$  is nonzero.

From this value we find that

$$\bar{y}^3 = \begin{cases} \left(\frac{1}{2\pi}\right)^2 \cdot \frac{\bar{N} \tilde{\Phi}_f(\omega_0, \omega_0)}{(2a)^3} \cdot \frac{27}{4} \left(a - \frac{2}{3}\omega_0\right)^2 & \text{for } a > \frac{2}{3}\omega_0 \\ 0 & \text{for } a < \frac{2}{3}\omega_0 \end{cases} \quad (53)$$

This sharp cutoff of the third moment at  $a = 2/3 \omega_0$  is the result of the idealization in the infinitely sharp cutoff of the network but it does provide information about the region of rapid approach to zero of the third moment for more realistic networks. Examination of the situation for the higher-order odd moments will provide an extension of this insight into the nature of the approach to a gaussian distribution.

Next we examine the third-order spectral density given by Eq. (47). If we eliminate the terms that incorporate  $\delta(\omega_1)$ ,  $\delta(\omega_2)$ ,  $\delta(\omega_3)$  or  $\delta(\omega_1 + \omega_2 + \omega_3)$ , we are left with

$$\begin{aligned} \Phi_y(\omega_1, \omega_2, \omega_3) = & [H(\omega_1) H(\omega_2) H(\omega_3) H^*(\omega_1 + \omega_2 + \omega_3)] \\ & \times \{ \bar{N} \tilde{\Phi}_f(\omega_1, \omega_2, \omega_3) + 2\pi \bar{N}^2 [\tilde{\Phi}_f(\omega_1) \tilde{\Phi}_f(\omega_3) \delta(\omega_2 + \omega_3) \\ & + \tilde{\Phi}_f(\omega_2) \tilde{\Phi}_f(\omega_3) \delta(\omega_1 + \omega_3) + \tilde{\Phi}_f(\omega_3) \tilde{\Phi}_f(\omega_2) \delta(\omega_1 + \omega_2)] \} \end{aligned} \quad (54)$$

Consider the contribution to  $\overline{y^4}$  from the first term in this function:

$$\overline{N} \tilde{\Phi}_f(\omega_1, \omega_2, \omega_3) H(\omega_1) H(\omega_2) H(\omega_3) H^*(\omega_1 + \omega_2 + \omega_3)$$

Corresponding to the  $\omega_1, \omega_2$  plane in the evaluation of the third moment we now have  $\omega_1, \omega_2, \omega_3$  space in which we must find the volume in which  $H(\omega_1) H(\omega_2) H(\omega_3) H^*(\omega_1 + \omega_2 + \omega_3)$  is nonzero. For  $H(\omega_1) H(\omega_2) H(\omega_3)$  there are eight cubes with sides of length  $\alpha$  centered at the eight points specified by  $(\pm\omega_0, \pm\omega_0, \pm\omega_0)$ . When the further requirement that  $H^*(\omega_1 + \omega_2 + \omega_3)$  be nonzero is added, the cubes at  $(+\omega_0, +\omega_0, +\omega_0)$  and  $(-\omega_0, -\omega_0, -\omega_0)$  are eliminated and the other six cubes are reduced in volume. The solid that remains at  $(\omega_0, \omega_0, -\omega_0)$  is shown in Fig. 3. The volume of the solid is  $\alpha^3/2$ . It should be noted that if  $\tilde{\Phi}_f(\omega_1, \omega_2, \omega_3)$  takes on the value  $\tilde{\Phi}_f(\omega_0, -\omega_0, \omega_0)$  throughout the volume centered at  $(\omega_0, -\omega_0, \omega_0)$ , it will take on this value within each of the other five solids because

$$\tilde{\Phi}_f(\omega_0, -\omega_0, \omega_0) = F(\omega_0) F^*(\omega_0) F(\omega_0) F^*(\omega_0)$$

Therefore, this first term in the third-order spectral density of the input gives a contribution  $\frac{1}{(2\pi)^3} \frac{3\overline{N}}{16\alpha} \tilde{\Phi}_f(\omega_0, -\omega_0, \omega_0)$  to  $\overline{y^4}$ .

Examination of the symmetries involved in the second term in  $\Phi_y(\omega_1, \omega_2, \omega_3)$  shows that three equal results will be obtained. Therefore, we now consider only the first of these three terms. We seek to evaluate

$$\left(\frac{1}{2\pi}\right)^3 \iiint_{-\infty}^{\infty} 2\pi \overline{N}^2 \tilde{\Phi}_f(\omega_1) \tilde{\Phi}_f(\omega_3) \delta(\omega_2 + \omega_3) H(\omega_1) H(\omega_2) H(\omega_3) H^*(\omega_1 + \omega_2 + \omega_3) d\omega_1 d\omega_2 d\omega_3$$

Integration with respect to  $\omega_2$  yields

$$\left(\frac{\overline{N}}{2\pi}\right)^2 \iint_{-\infty}^{\infty} \tilde{\Phi}_f(\omega_1) \tilde{\Phi}_f(\omega_3) H(\omega_1) H^*(\omega_3) H(\omega_3) H^*(\omega_1) d\omega_1 d\omega_3$$

which reduces to

$$\left[ \frac{\overline{N}}{2\pi} \frac{\tilde{\Phi}_f(\omega_0)}{2\alpha} \right]^2$$

Now, we can write for the fourth moment:

$$\overline{y^4} = \frac{3\overline{N}}{(2\pi)^3 (16\alpha)} \tilde{\Phi}_f(\omega_0, -\omega_0, \omega_0) + 3 \left[ \frac{\overline{N}}{2\pi} \frac{\tilde{\Phi}_f(\omega_0)}{2\alpha} \right]^2 \quad (55)$$

The skewness and excess (19) are

$$\gamma_1 = \frac{\overline{y^3}}{(\overline{y^2})^{3/2}} = \begin{cases} \frac{27}{4} \sqrt{\frac{1}{2\pi\overline{N}}} \frac{\tilde{\Phi}_f(\omega_0, \omega_0)}{[\tilde{\Phi}_f(\omega_0)]^{3/2}} \frac{\left(\alpha - \frac{2}{3}\omega_0\right)^2}{(2\alpha)^{3/2}} & \text{for } \alpha > \frac{2}{3}\omega_0 \\ 0 & \text{for } \alpha < \frac{2}{3}\omega_0 \end{cases} \quad (56)$$

and

$$\gamma_2 = \frac{\overline{y^4}}{(\overline{y^2})^2} - 3 = \frac{3\alpha}{8\pi\overline{N}} \frac{\tilde{\Phi}_f(\omega_0, -\omega_0, \omega_0)}{[\tilde{\Phi}_f(\omega_0)]^2} = \frac{3\alpha}{8\pi\overline{N}} \quad (57)$$

Next we examine the behavior of the  $n^{\text{th}}$ -order moments, considering the behavior for  $n$  even and  $n$  odd separately.

The moment of order  $n$  (for  $n$  even) will be derived from the  $n-1^{\text{th}}$ -order auto-correlation function.

$$\phi_x(\tau_1, \tau_2, \dots, \tau_{n-1}) = \lim_{T \rightarrow \infty} \frac{1}{2T} \int_{-T}^T \left[ \sum_{m_0=1}^N f(t - t_{m_0}) \right] \left[ \sum_{m_1=1}^N f(t - t_{m_1} + \tau_1) \right] \dots \left[ \sum_{m_{n-1}=1}^N f(t - t_{m_{n-1}} + \tau_{n-1}) \right] \quad (58)$$

There are, then,  $n$  indices to be considered. If there are any cases in which a single index differs from all the others, a  $\delta(\omega_m)$  term will appear. Such cases, then, will provide no contribution to the  $n^{\text{th}}$ -order moment and so need not be considered. Now suppose that there are  $a$  different indices available. Then we can see the general form of the term in Eq. (48). If we multiply this by  $H(\omega_1) \dots H(\omega_{n-1}) H^*(\omega_1 + \dots + \omega_{n-1})$  and integrate with respect to the  $n-1^{\text{th}}$  variables, we obtain a result of the order of  $1/\alpha^a$ . Since our interest centers on the normalized  $n^{\text{th}}$  moment, which is  $\mu_n/(\mu_2)^{n/2}$  and is of the order  $\mu_n \alpha^{n/2}$ , we must consider the behavior of  $\alpha^{(n/2)-a}$ . This will be a constant for  $a = n/2$ , which implies that when the number of different indices is equal to  $n/2$ , there is a contribution to  $\overline{y^n}$  which is independent of  $\alpha$ . Since no indices may appear less than twice, this specifies that, for  $\alpha \rightarrow 0$ , the only terms in  $\Phi_x(\omega_1 \dots \omega_{n-1})$  that contribute are those of the form

$$[\tilde{\Phi}_f(\omega_1)][\tilde{\Phi}_f(\omega_3) \delta(\omega_2 + \omega_3)][\tilde{\Phi}_f(\omega_5) \delta(\omega_4 + \omega_5)] \dots [\tilde{\Phi}_f(\omega_{n-1}) \delta(\omega_{n-2} + \omega_{n-1})]$$

The number of such terms is equal to the number of different selections that can be made among  $n$  indices, taken two at a time, and it equals  $(n-1)(n-3) \dots 5 \cdot 3 \cdot 1$ , which is precisely the value of the normalized gaussian  $n^{\text{th}}$  moment. The terms of next higher order in  $\alpha$  will have  $(n/2)-1$  different indices (all appearing twice except one which appears four times). They will make a contribution to the normalized moment of order  $\alpha$  and will go to zero directly with the bandwidth. Other terms will be of higher order in  $\alpha$  up to  $\alpha^{(n/2)-1}$  for the case in which all indices are identical.

Next consider the  $n^{\text{th}}$ -order normalized moment, where  $n$  is odd. There are  $n$  indices in this case but since every index must appear more than once, there can, at most, be  $(n-1)/2$  different indices. This would yield a term of order

$$\frac{\left(\alpha - \frac{2}{3} \omega_0\right)^2}{\alpha^{3/2}}, \text{ which exists only for } \alpha > \frac{2\omega_0}{3}. \text{ The term of next higher order}$$

is of order  $\frac{\left(\alpha - \frac{2}{5} \omega_0\right)^4}{\alpha^{5/2}}$  and will be nonzero for  $\alpha > \frac{2\omega_0}{5}$ . We can describe the situation for the  $n^{\text{th}}$  moment as  $\alpha$  increases from zero. When  $\alpha = \frac{2\omega_0}{n}$ , the  $n^{\text{th}}$  moment becomes nonzero. It now increases proportional to  $\frac{\left(\alpha - \frac{2}{n} \omega_0\right)^{n-1}}{\alpha^{n/2}}$ . When  $\alpha$  reaches the value  $\frac{2\omega_0}{n-2}$ , another series of terms comes into existence which is of order  $\frac{\left(\alpha - \frac{2\omega_0}{n-2}\right)^{n-3}}{\alpha \frac{n-2}{2}}$ . This process continues until  $\alpha \geq \frac{2\omega_0}{3}$ , when all the non-dc

terms will have appeared. It is clear, then, that however narrow we make the bandwidth, some higher-order odd moments will exist.

This application of the moments technique in the frequency domain has shed some light on the nature of the approach to gaussian statistics with narrow-band filtering, in addition to providing a proof of this approach to supplement the usual Central-Limit-Theorem proof.

### 3.3 THE EFFECT OF LOW-FREQUENCY FILTERING ON RANDOM-PULSE NOISE: AN APPLICATION OF THE MOMENTS TECHNIQUE IN THE TIME DOMAIN

The effect of an RC low-frequency filter on the amplitude distribution of a sum of random pulses can be found by evaluation of the moments in the time domain. The result will have significance for the question of how much of the low-frequency energy of a physical noise process can be filtered out if we are interested in determining the form of the amplitude probability distribution of a physical (possibly non-gaussian) noise.

We take, as a particularly illuminating example of a noise process, a train of unit steps with Poisson-distributed starting times. We seek information about the amplitude probability density of the output from a linear filter whose system function is

$$H(s) = \frac{1}{\tau_0} \frac{s}{\left(s + \frac{1}{\tau_0}\right)\left(s + \frac{1}{\tau}\right)} \quad (59)$$

This system function corresponds to the filtering imposed by a typical measuring system whose response falls off at 20 db per decade both at high and low frequencies. We shall allow  $\tau$  to vary while  $\tau_0$  is held fixed so that for  $\tau < \tau_0$  we have a constant low-frequency cutoff and a variable high-frequency limit, while, for  $\tau > \tau_0$ , it is the low-frequency cutoff that is variable.

The response of this network to a unit step is

$$e(t) = \frac{\tau}{\tau - \tau_0} (e^{-t/\tau} - e^{-t/\tau_0}) \quad (t > 0) \quad (60)$$

It should be noted that  $H(s)$  is unity for the middle-frequency region, if  $\tau$  is the low-frequency pole ( $\tau > \tau_0$ ), but is not unity, if  $\tau$  is the high-frequency pole. We shall consider the normalized moments, however, so that this will make no difference in our results.

We use Eq. (30) to establish an expression for the  $m^{\text{th}}$  semi-invariant.

$$K_m = \bar{N} \int_0^\infty [e(t)]^m dt \quad (61)$$

Performing the indicated integration, we obtain the general expression:

$$K_m = \bar{N} \left( \frac{\tau}{\tau - \tau_0} \right)^m \sum_{\ell=0}^m \frac{(-1)^\ell m!}{(m-\ell)! \ell!} \frac{\tau \tau_0}{(m-\ell) \tau_0 + \ell \tau} \quad (62)$$

We evaluate the first four semi-invariants (17) and obtain from them expressions for the skewness  $\gamma_1$  and the excess  $\gamma_2$  which will be examined in greater detail.

$$K_1 = \bar{N} \tau \quad K_2 = \frac{\bar{N} \tau^2}{2(\tau_0 + \tau)} \quad K_3 = \frac{2\bar{N} \tau^3}{3(\tau_0 + 2\tau)(2\tau_0 + \tau)}$$

$$K_4 = \frac{3\bar{N} \tau^4}{4(\tau_0 + \tau)(3\tau_0 + \tau)(\tau_0 + 3\tau)}$$

$$\gamma_1 = \frac{K_3}{K_2^{3/2}} = \frac{1}{\sqrt{\bar{N}}} \frac{1}{\frac{3(\tau_0 + 2\tau)(2\tau_0 + \tau)}{4\sqrt{2}(\tau_0 + \tau)^{3/2}}} \quad (63)$$

$$\gamma_2 = \frac{K_4}{K_2^2} = \frac{1}{\bar{N}} \frac{1}{\frac{(3\tau_0 + \tau)(\tau_0 + 3\tau)}{3(\tau_0 + \tau)}} \quad (64)$$

The skewness and excess are plotted in Fig. 4. It is clear that it is the low-frequency pole which modifies the probability distribution of the sum of Poisson-distributed unit steps most markedly. Furthermore, as the system eliminates an increasing portion of the low-frequency energy, the distribution deviates increasingly from gaussian. This indicates the need for clarification of any broad statement which maintains that: as the bandwidth in which a non-gaussian noise is examined goes to zero, the amplitude probability distribution goes to gaussian. This statement does not apply in the above case because the skirts of the system function are not sharp enough. Evidently some property of the skirts must be included in the "band-limiting" statement.

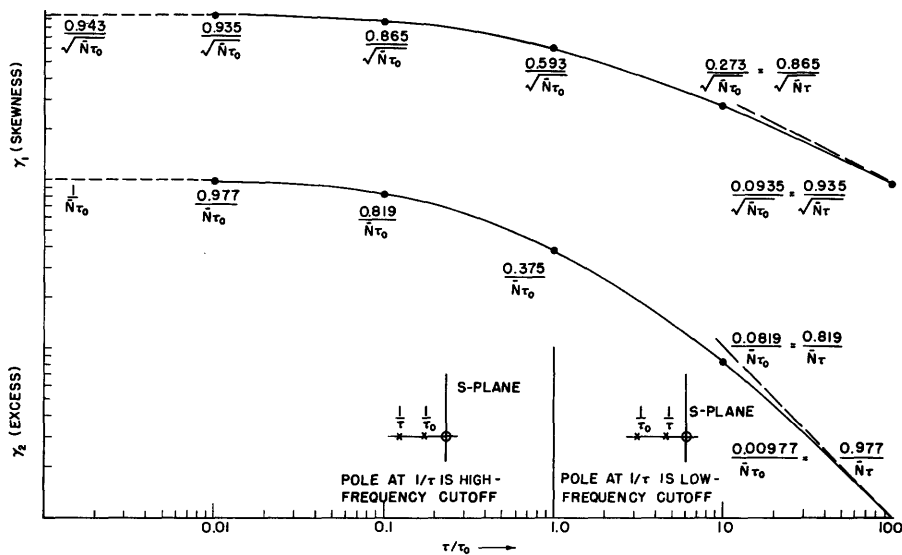


Fig. 4. Effect on the skewness and excess of moving a pole of  $H(s)$ .

The necessary clarification can be obtained by restating the criterion for approach to a gaussian distribution as follows: For a progressively longer filter memory, a filtered non-gaussian noise approaches a gaussian distribution. By limiting the low-frequency response in the manner considered in the example above, we actually reduce the memory of such a nonoscillatory system. Middleton (14) points out that

the amount of overlapping in a sum of random pulses provides a good criterion for the deviation from a gaussian distribution. This viewpoint is certainly reasonable on the basis of Central-Limit-Theorem ideas, and it evidently applies to the case of pulses modified by passing through a linear network. In that case, the amount of overlapping at the output clearly becomes a function of both the overlapping of the original input pulses and the memory of the filter.

In relation to experimental methods of measuring the probability distribution of noises for which the sum of randomly occurring pulses is the model, it is clear from the foregoing that "eliminating the low-frequency energy" can often lead to measurements that are farther from gaussian than is the actual noise distribution.

## IV. SEMICONDUCTOR NOISE MEASUREMENTS

### 4.1 MEASUREMENTS AND TECHNIQUES

The nature of the measurements of  $1/f$  noise in germanium junction diodes and of avalanche noise in silicon junction diodes will now be discussed and an estimate of the expected error in these measurements provided. A brief description of the moments-measurement equipment is given here; for a more complete description see reference 9.

Four measurements were made on semiconductor noise:

1. The second, third, and fourth moments were evaluated experimentally.
2. The frequency spectrum was measured between 100 cps and 60 kc.
3. Photographs of the noise waveforms were taken.
4. Probabiloscope photographs were taken to provide a qualitative picture of the distribution density.

The measuring system is shown in Fig. 5.

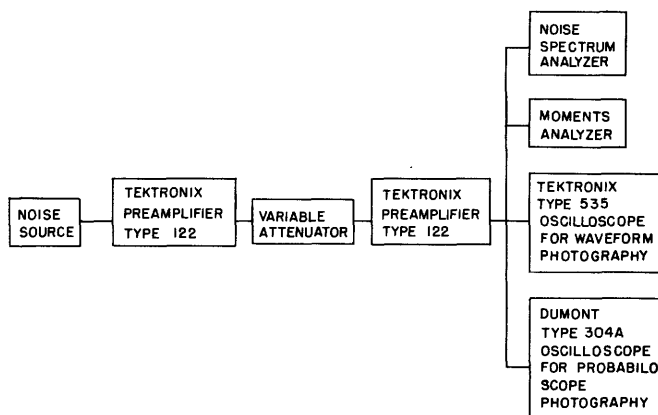


Fig. 5. Over-all measuring system.

The noise source consisted of the diode under examination in a constant temperature bath and a suitable biasing circuit. This noise source is shown in Fig. 6. For the 1N91 diode, measurements were made at room temperature. The constant temperature bath in this case was one pint of water in a Dewar flask. Since measurements were taken every half hour, it was felt that the high heat capacity of the bath and the

low thermal heat transfer into the Dewar flask would result in temperature variations so small that the moments measurements would not be affected. Application of Newton's law of cooling to available data (20) gives an expected change of  $0.1^{\circ}\text{C}$  for a  $5^{\circ}\text{F}$  temperature differential over one-half hour. The silicon diode noise was measured at the equilibrium temperature of a mixture of dry ice and acetone. This mixture in a Dewar flask provided a constant temperature environment.

The noise spectrum analyzer (21) is a heterodyne analyzer with filter bandwidths of 10 cps and 100 cps. It provides continuous measurements of the noise spectrum between 100 cps and 60 kc.

A Tektronix 535 oscilloscope and a 35-mm oscilloscope camera were used to photograph single stroke traces of the noise. The brightness of the oscilloscope spot was increased in proportion to the rate of travel by an intensifier as described by Kemp (22).

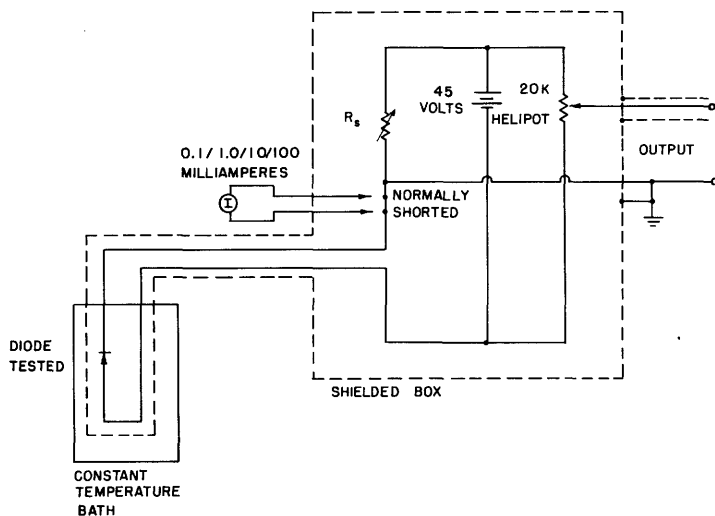


Fig. 6. Noise source.

cathode-follower unit which fed three function generators whose outputs were proportional to the square, cube, and fourth power of the noise. Three integrators then provided the desired moment values.

The amplifier-rectifier-cathode-follower unit provided a gain of approximately eight from a paraphase amplifier so that the second Tektronix preamplifier would not operate in a nonlinear region. It was found simpler to design a full-wave rectifier to feed the square- and fourth-power function generators than to design function generators with the desired accuracy of balance. The full-wave rectifier was balanced to 1 per cent. The cathode followers in this unit had output impedances of the order of 100 ohms. The frequency response of these units was good at 40 kc.

The function generators used back-biased diodes to match straight line segments to the desired power laws. The desired accuracy was  $\pm 2$  per cent of the desired value over output amplitude ranges of 50:1, 125:1, and 256:1 for the square-, cube-, and fourth-power units. They are dc units so that the minimum amplitudes in these ranges are set by the function-generator drift and the drift of the integrator input circuit. The frequency response of the over-all function-generator system, including the amplifier-rectifier-cathode-follower unit, is good to 10 kc.

The integrators were designed to average the input function with a 10-second time constant, and then apply this average to drive watt-hour meters. The only limitation on the length of the integration period is the drift of the input circuits. However, the ease of taking readings every half-hour (and resetting the zero) led us to do so in this study. In a half-hour period, the over-all moments analyzer drift was less

The probabiloscope (23) used a DuMont 304A oscilloscope with a 5ADP15 tube, a 35-mm oscilloscope camera, and an optical wedge with a density range of 1:3 (a fractional transmission range of 1000:1). No attempt was made to evaluate numerically the probability distribution, since the intention was to obtain a qualitative picture of the distribution for comparison with the result from the moments.

The moments analyzer (Fig. 7) consisted of an amplifier-rectifier-

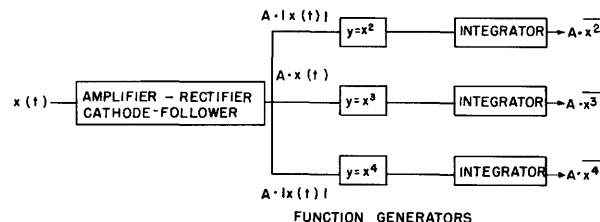


Fig. 7. Moments analyzer.



than 10 mv at the input to the chopper circuit in the integrator. The accuracy of the integrators is of the order of  $\pm 3$  per cent except for very small inputs.

#### 4.2 ERRORS RESULTING FROM LENGTH OF OBSERVATION TIME

In addition to the errors in measuring the moments inherent in the particular types of function generators and integrators that were used, there are unavoidable errors caused by the limited observation time and by the limited amplitude range that can be incorporated in the function generators. The limited observation time is particularly significant when an attempt is being made to measure the amplitude probability distribution of noise with a  $1/f$  spectral density, owing to the long correlation times that are required.

Consider an ensemble of stationary ergodic random functions. We want to measure some property of this ensemble by observing one member of it for a period of time  $T$ . If we performed this operation on each member of the ensemble, we would obtain a series of values that are random functions. We want to estimate the variance of these values in order to determine how accurately a measurement that is made on one member represents the average value for the ensemble. In the limit  $T \rightarrow \infty$  the value for one member must approach the average value for the ensemble (from the ergodic property). For the case of  $1/f$  noise, we shall be interested in measuring the moments of a random function which, it develops, actually has a gaussian or near-gaussian distribution. For such distributions, the contribution to the measured average from extreme values increases as we consider higher-degree moments. Therefore, we would expect to find that a longer observation time is required for the fourth moment than for the second, and, indeed, this is true. The development of the results below is based on a theory of statistical errors in measurements on random time functions developed by Costas (24), Davenport, Johnson, and Middleton, (25), and Siegert (26).

We wish to measure the average value of a function of a random variable,  $x(t)$ . Let us define  $z(t)$  as

$$z(t) = g[x(t)] \quad (65)$$

We are, then, interested in the properties of

$$M(T) = \frac{1}{T} \int_0^T z(t) dt \quad (66)$$

In this study we shall examine the mean and the variance of  $M(T)$ , using the method described in reference 25.

The ensemble average is

$$\overline{M(T)} = \overline{\frac{1}{T} \int_0^T z(t) dt} = \bar{z} \quad (67)$$

This is expected, since the ensemble is stationary. The variance of  $M(T)$  is

$$\sigma_M^2(T) = \frac{2}{T} \int_0^T \left(1 - \frac{\tau}{T}\right) [\phi_z(\tau) - \bar{z}^2] d\tau \quad (68)$$

Now consider the evaluation of  $\phi_z(\tau)$  for the first four moments in terms of  $\phi_x(\tau)$ . For  $z = x$  we see immediately that

$$\phi_z(\tau) = \phi_x(\tau) \quad (69)$$

For  $z = x^2$  we wish to evaluate  $\overline{z_1 z_2} = \overline{x_1^2 x_2^2}$ , where  $x_1 = x(t)$  and  $x_2 = x(t + \tau)$ . We now specify that  $x(t)$  obey a gaussian distribution law. Although this limits the results somewhat, they still can serve as a guide for the case in which  $x(t)$  is nearly gaussian. We can, from Eq. (6), write

$$\overline{x_1^2 x_2^2} = (j)^4 \left. \frac{\partial^4 F_x(u_1, u_2)}{\partial u_1^2 \partial u_2^2} \right]_{u_1=u_2=0} \quad (70)$$

For a gaussian distribution,

$$F_x(u_1, u_2, \dots, u_m) = \exp \left\{ -\frac{1}{2} \left[ \sum_{k=1}^m \sum_{\ell=1}^m \phi_x(t_\ell - t_k) u_\ell u_k \right] + j \sum_{k=1}^m \bar{x}_k u_k \right\} \quad (71)$$

We take  $\bar{x} = 0$ , since the equipment used in this investigation did not pass dc. If we perform the indicated operation on  $F_x(u_1, u_2)$ , we obtain

$$\phi_z(\tau) = \overline{x_1^2 x_2^2} = \sigma_x^4 + 2 \phi_x^2(\tau) \quad (72)$$

We can use the same technique in order to get the correlation functions of the other moments. We list the results for the second, third, and fourth moments:

$$\phi_{x^2}(\tau) = 2 \phi_x^2(\tau) + \sigma_x^4 \quad (73)$$

$$\phi_{x^3}(\tau) = 6 \phi_x^3(\tau) + 9 \sigma_x^4 \phi_x(\tau) \quad (74)$$

$$\phi_{x^4}(\tau) = 24 \phi_x^4(\tau) + 72 \phi_x^2(\tau) + 9 \sigma_x^8 \quad (75)$$

Consider first the simple case in which

$$\phi_x(\tau) = \sigma_x^2 e^{-|\tau|/\tau_0} \quad (76)$$

This is the case for which

$$\Phi_x(\omega) = \frac{2}{\tau_0} \frac{\sigma_x^2}{\omega^2 + \frac{1}{\tau_0^2}} \quad (77)$$

where  $\sigma_x^2$  is the ensemble-wise variance of  $x(t)$ .

Now we can obtain values for  $\sigma_x^2(T)$ ,  $\sigma_{x^2}^2(T)$ ,  $\sigma_{x^3}^2(T)$ , and  $\sigma_{x^4}^2(T)$  from Eq. (68). We assume  $T \gg \tau_0$ . Then we obtain

$$\sigma_x^2(T) = \frac{2\tau_0}{T} \sigma_x^2 \quad (78)$$

$$\sigma_{x^2}^2(T) = \frac{2\tau_0}{T} \sigma_x^4 \quad (79)$$

$$\sigma_{x^3}^2(T) = \frac{22\tau_0}{T} \sigma_x^6 \quad (80)$$

$$\sigma_{x^4}^2(T) = \frac{84\tau_0}{T} \sigma_x^8 \quad (81)$$

We have now obtained two properties of the distribution of the first four moments of a sample taken in time  $T$ : the mean and the variance. It is clear that  $z(t) = [x(t)]^n$  does not have a gaussian distribution. However, the operation of integration for a period  $T$  can be thought of as passing  $[x(t)]^n$  through a filter whose memory is  $T$ . This, as we have seen in section 3.3, leads to an approach towards gaussian statistics at the output of such a filter. To a good approximation, therefore, we can assume a nearly gaussian distribution of the sample statistics. If  $M(T)$  obeyed a gaussian distribution, the probability of a single value lying within the  $\pm 2\sigma_M$  limits would be 95 per cent. We can establish a criterion for a suitable observation period,  $T$ , then, on the basis that  $2\sigma_M = 0.05\overline{M}$ .

In Table I expressions for  $\sigma_{x^n}^2(T)$ ,  $\overline{x^n}$ , and the value for  $T$ , using this criterion for the case when the autocorrelation function  $\phi_x(\tau) = \sigma_x^2 e^{-\tau/\tau_0}$ , are given. For the third moment, we have substituted  $|\overline{x^3}|$  (the third absolute moment) for  $\overline{x^3}$  so that the criterion can be applied.

Table I. Observation Times Required for 95 Per Cent Probability of Less than 5 Per Cent Error.			
Moment (n)	$\sigma_{x^n}^2 (T)$	$\overline{x^n}$	T
2	$2 \frac{\tau_0}{T} \sigma_x^4$	$\sigma_x^2$	$3200 \tau_0$
3	$22 \frac{\tau_0}{T} \sigma_x^6$	$2 \sqrt{\frac{2}{\pi}} \sigma_x^3$	$13,800 \tau_0$
4	$84 \frac{\tau_0}{T} \sigma_x^8$	$3 \sigma_x^4$	$15,000 \tau_0$

Now we recall that the frequency spectrum of  $x(t)$  that was chosen in the above case Eq. (77) is flat up to a high-frequency cutoff at  $1/2\pi\tau_0$  cps. In this study, however, we are interested in making measurements on functions that have  $1/f$  spectra. We filter this noise at both low and high frequencies before measurements are made (0.2 cps and 10 kc) so that, for the measured function, the spectral density can be approximated by

$$\Phi_x(\omega) \cong \frac{|\omega|}{(\omega^2 + \omega_1^2)(\omega^2 + \omega_2^2)} \quad (82)$$

where  $\omega_1$  is the low-frequency system cutoff and  $\omega_2$  the high-frequency cutoff. The autocorrelation function corresponding to this spectral density can be found in terms of the exponential integral function by using relations given by Jahnke and Emde (27).

$$\phi_x(\tau) = \frac{1}{\omega_2^2 - \omega_1^2} [e^{+\tau\omega_2} E_i(-\tau\omega_2) + e^{-\tau\omega_2} \overline{E}_i(\tau\omega_2) - e^{+\tau\omega_1} E_i(-\tau\omega_1) - e^{-\tau\omega_1} \overline{E}_i(\tau\omega_1)] \quad (83)$$

This function is plotted in Figs. 8 and 9. However, in this case, we cannot obtain the values of  $\sigma_z^2(T)$  by direct integration.

We shall now establish a criterion for the observation time that is necessary to achieve suitable fourth-moment accuracy when gaussian noise with a  $1/f$  spectrum is observed. In the integration for  $\sigma_{x^4}^2(T)$ , the major contribution comes from small values of the argument ( $\tau$ ). The extension of the integration to  $15000 \tau_0$  was made so that the  $2/T$  coefficient would become small, but the contribution to  $\sigma_{x^4}^2(T)$  for  $\tau \gg \tau_0$  is negligible.

Therefore, we compare the values of  $\int_0^T (1 - \tau/T) [\phi_z(\tau) - \bar{z}^2] d\tau$  for the exponential autocorrelation function and for the exponential integral function. We have seen Eq. (81) that, for the exponential, we obtain  $42 \tau_0 \sigma_x^8$ . If we use numerical

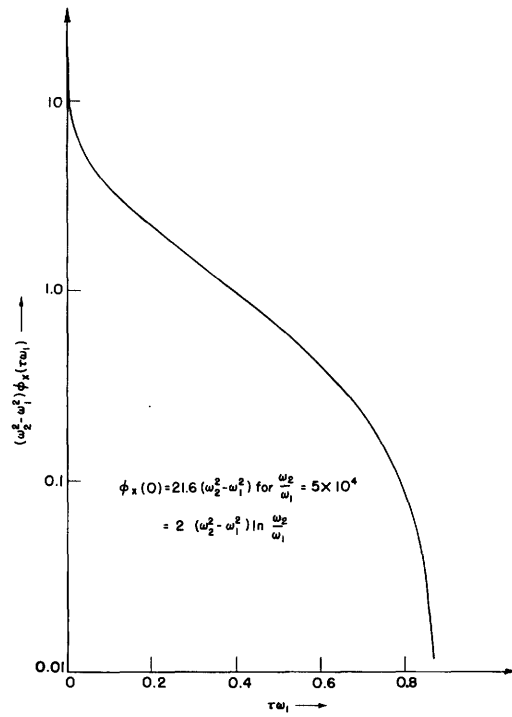


Fig. 8. Autocorrelation function of 1/f noise, RC filtered at high and low frequencies drawn for small values of the argument.

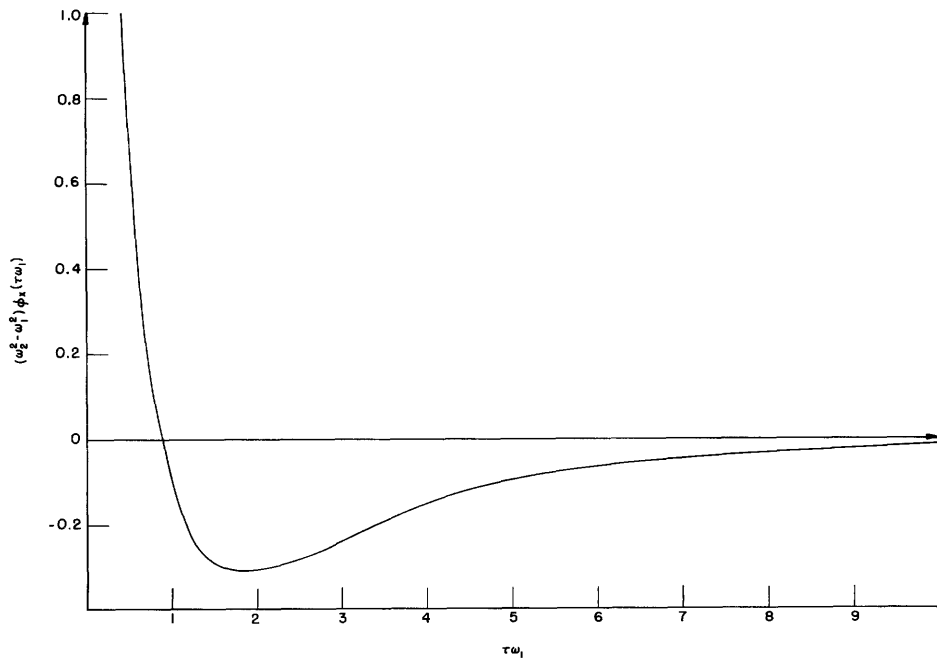


Fig. 9. Autocorrelation function for large values of the argument.

integration when  $\tau\omega_1$  is small and an analytic expression for the proper asymptotic series (28) for the exponential-integral function when  $\tau\omega_1$  is large, we obtain  $(1.17) \times (\sigma_x^8/\omega_1)$  ( $\omega_2/\omega_1$  is taken to be 50,000, as it was in this investigation). Therefore, an appropriate parameter for use in the  $T = 15,000 \tau_0$  equation would seem to be

$$\tau_0^1 = \frac{1.17}{42} \cdot \frac{1}{\omega_1} = \frac{0.028}{\omega_1}$$

Since this development (especially the numerical integration) is quite approximate, an arbitrary factor of 10 is now inserted in this criterion. Therefore,

$$\tau_0^1 = \frac{0.28}{\omega_1}$$

Our requirement of 95 per cent probability of an error of less than 5 per cent for the fourth moment, when  $\omega_1 = 2\pi \times 0.2$  cps, is

$$T \cong 1 \text{ hour} \tag{84}$$

The measurements on 1/f excess noise were actually made at 30-minute intervals over a 30-hour period. It is felt that the standard deviation of these individual measurements is about evenly divided between the errors caused by the components of the moments-measurement system and the errors arising from the length of observation time.

#### 4.3 ERRORS RESULTING FROM A LIMITED AMPLITUDE RANGE

Next we consider the effect of limitations in the amplitude range of the function generators that were used to obtain the square, cube, and fourth powers of the input noise. For large amplitudes, the contribution to the integrated values of the moment is large but the probability of occurrence is small. We must, therefore, concern ourselves with the area under the curve defined by  $x^n p(x)$ . The total area is the value of the moment but the height of the curve  $x^n p(x)$  is proportional to the contribution at any amplitude. In order to get a clearer picture of the requirements to be imposed on the equipment design, however, the cumulative area under these curves is examined in Fig. 10. We can tabulate the five and ninety-five per cent values from this curve (see Table II). Within these values, we wish to obtain 2 per cent accuracy. It is clear that the most stringent output dynamic-range accuracy requirement will be on the fourth-moment generator. The chosen dynamic range must be greater than that from five to ninety-five per cent because it is difficult to center the input amplitude range precisely with respect to the accurate portion of the function-generator characteristic. In particular, we designed for a usable fourth-moment input amplitude range of 4:1 or an

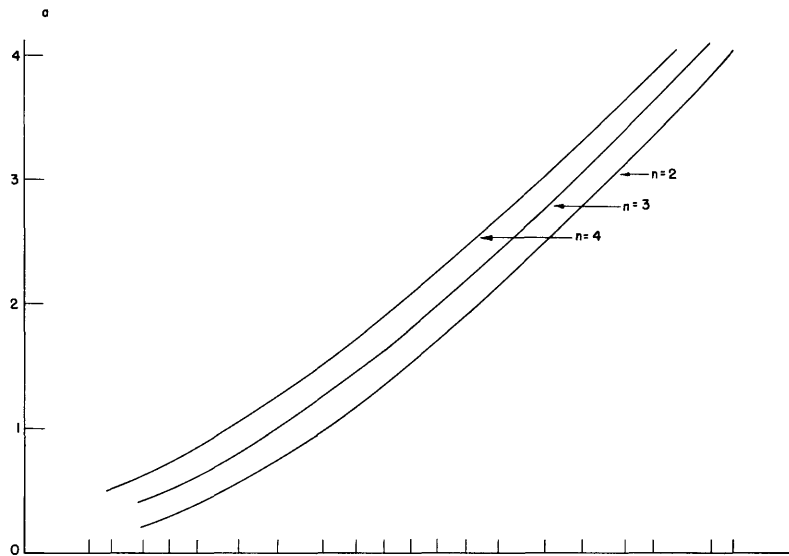


Fig. 10. Plot of  $100 \left( \frac{\int_0^a x^n p(x) dx}{x^n} \right)$  for a normalized gaussian variable.

Table II. The 5 and 95 Per Cent Values for $\frac{\int_0^a x^n p(x) dx}{x^n}$ .		
n	<u>5th per cent of moment</u>	<u>95th per cent of moment</u>
	a	a
2	0.58	2.78
3	0.82	3.05
4	1.06	3.32

output range of 256:1. For the third-moment generator, a 5:1 input or a 125:1 output range is called for. For the second moment, we require a 7:1 input range, since errors in the value of the second moment result in an error twice as large in the evaluation of the excess. This corresponds to a 50:1 output range.

The design criteria in these last sections are based on limiting each error to 5 per cent. However, the design incorporates several conservative factors, and actual checks on known distributions (sine waves and square waves) lead us to believe that our results are of better than 5 per cent accuracy.

#### 4.4 MEASUREMENTS OF 1/f EXCESS NOISE

Measurements were made on a General Electric Company 1N91 germanium junction diode at room temperature. The back current was approximately 100  $\mu$ a for all

measurements and  $R_s$  was a 50-k wire-wound resistor. The noise voltage was approximately 20 millivolts, as measured by a Ballantine Model 300 averaging vacuum-tube voltmeter, in the frequency range 10 cps-40 kc and after amplification by a factor of 100 in the first preamplifier.

The spectral density of this noise was obtained; it is shown in Fig. 11. These

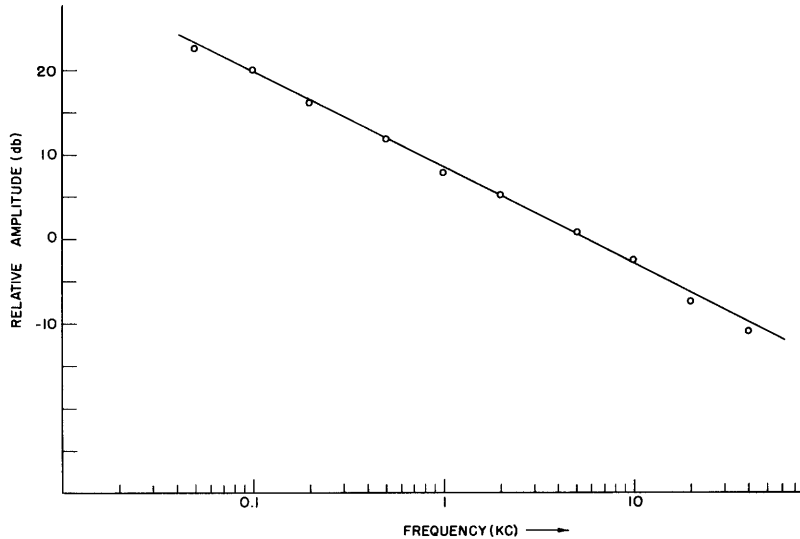


Fig. 11. Measured spectral density of 1N91 germanium diode noise.

data obey a  $1/f^{1.1}$  law, which is in agreement with the usual experimental measurements that give exponents varying from 1.0 to 1.4.

The moments of this noise were measured for 30 hours, readings being taken every half-hour. The frequency range that was examined was 0.2 cps-10 kc. The value for  $\mu_4/\mu_2^2$  was 2.88, as measured on the panel meters, with a standard deviation of 3.6 per cent, and 3.03, as measured by the integrators, with a

standard deviation of 3.6 per cent. The deviation from a gaussian distribution is clearly within the limits of experimental accuracy.

The values for  $\mu_3/\mu_2^{3/2}$  are +0.030, with a standard deviation of 130 per cent from panel meter readings, and +0.031, with a standard deviation of 62.5 per cent for the integrators. If we compare these values with  $|\overline{x^3}|/\mu_2^{3/2} = 1.6$  for rectified gaussian noise, we find that these values deviate from zero by less than 2 per cent. These deviations from gaussian noise are well within the expected experimental error of 5 per cent.

Photographs of the noise waveform for two sweep speeds are shown in Fig. 12. The probabloscope photograph for this noise is shown in Fig. 13. It displays the expected gaussian shape on a log-probability scale. A log-probability gaussian distribution curve is shown with it for comparison.

We conclude that  $1/f$  excess noise in germanium junction diodes has a gaussian first probability distribution.

#### 4.5 AVALANCHE NOISE

McKay (29) recognized that there was an increased noise from semiconductor diodes in the neighborhood of the inverse breakdown voltage and that this noise was



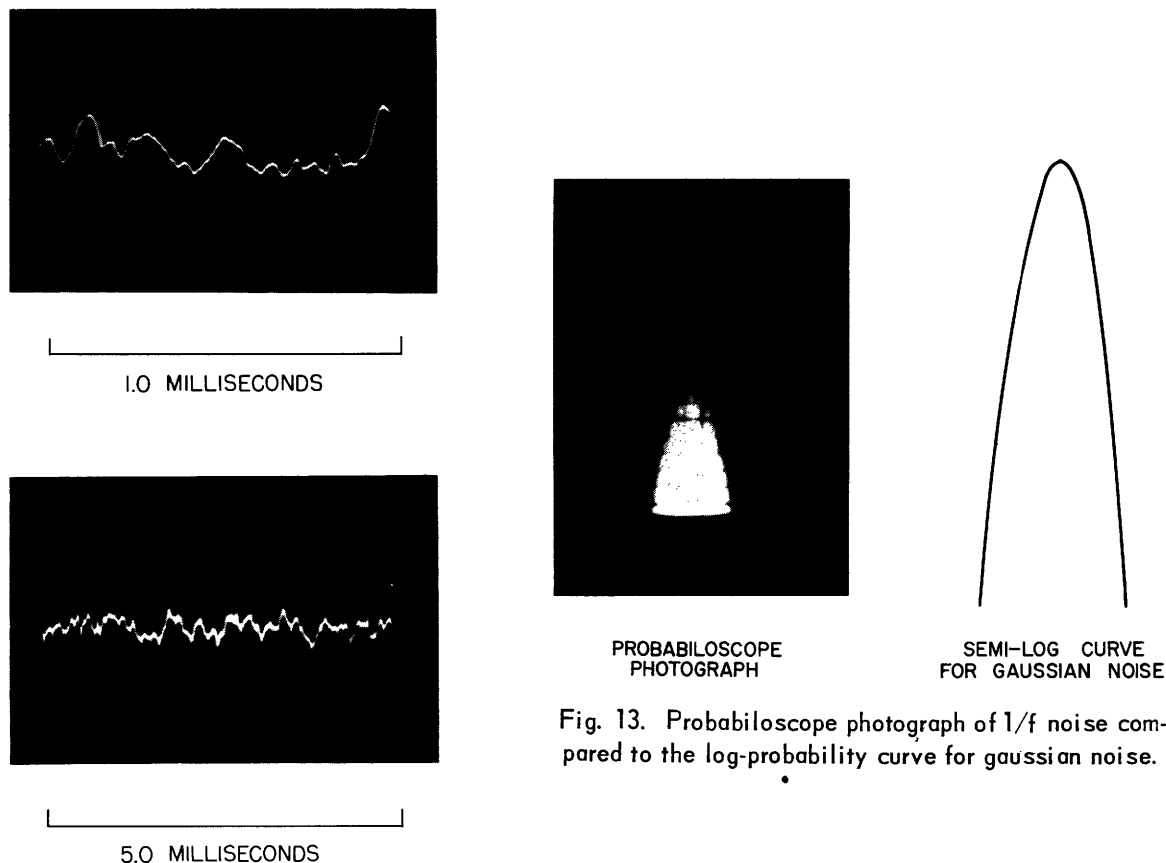


Fig. 13. Probabiloscope photograph of  $1/f$  noise compared to the log-probability curve for gaussian noise.

Fig. 12. Photographs of  $1/f$  noise waveforms.

visibly non-gaussian. We shall report some measurements made on this avalanche breakdown noise.

Measurements were made on a Raytheon Manufacturing Company 1N305A silicon junction diode that was held at the temperature of a mixture of dry ice and acetone ( $-77^{\circ}\text{C}$ ) for a range of inverse currents of  $27\ \mu\text{a}$  to  $500\ \mu\text{a}$ . The region of incipient breakdown is from below  $27\ \mu\text{a}$  to approximately  $160\ \mu\text{a}$ . Above  $160\ \mu\text{a}$  the diode was considerably less noisy.

Measurements of the spectral densities were made for several values of the reverse current in the avalanche region. These are shown in Fig. 14. We also present in Fig. 15 a spectral-density curve for a current that is well into the avalanche region ( $500\ \mu\text{a}$ ). It is clear from these curves that the noise is no longer  $1/f$  in nature and that, therefore, the averaging time for moments measurements could be considerably reduced.

Several five-hour runs were made and the resulting values for the moments from the integrator were compared to those from the panel meters on the integrator strips. It was found that deviations were well within the experimental error. We shall,

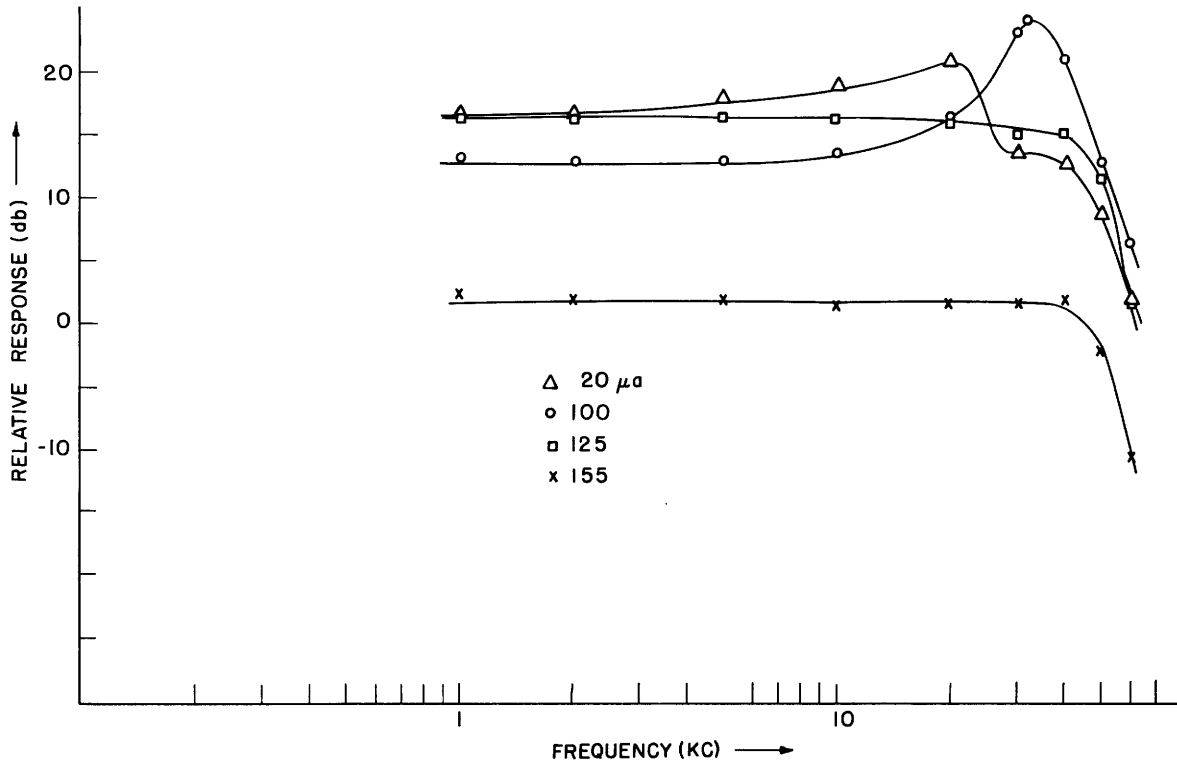


Fig. 14. Spectral densities of silicon junction diode avalanche noise for inverse currents of 20, 100, 125, and 155  $\mu a$ .

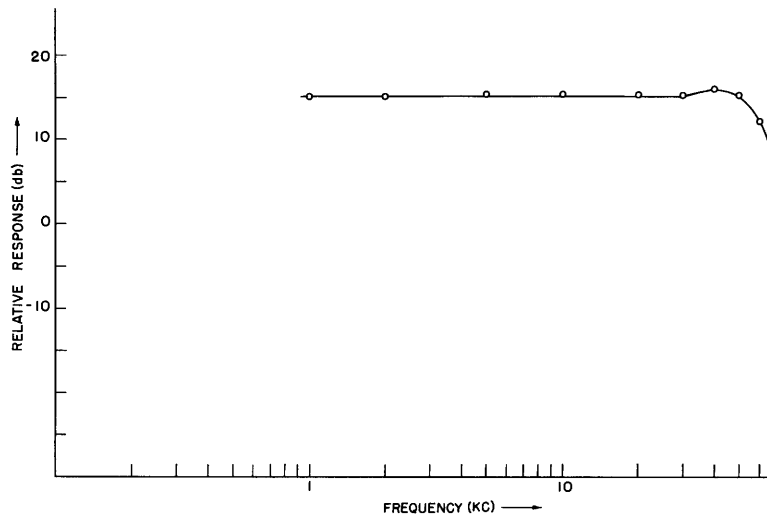


Fig. 15. Spectral density of avalanche noise for an inverse current of 500  $\mu a$ .

therefore, use these short-averaging-time moments in this section. For several values of the current, the frequency spectrum within which the measurements were made was varied in order to see the effect on the distribution. The expected approach to a gaussian distribution is demonstrated in this way. In Fig. 16 the effect of the high-frequency cutoff on the skewness and excess is shown for back currents of 90, 100, and 110  $\mu\text{a}$ . In Fig. 17 this approach to gaussian statistics is shown for 130, 140, and 150  $\mu\text{a}$ . The effect of variation of the back current in the avalanche region on the skewness and excess is shown in Fig. 18, in which all of the moments are measured in a bandwidth from 0.2 cps to 10 kc. Far into the avalanche region, at 500  $\mu\text{a}$  of back current, values of  $-0.007$  for the normalized third moment and  $2.88$  for the normalized fourth moment were obtained. These values are gaussian within the accuracy of the moments-measuring equipment.

Probabiloscope photographs were taken for back currents of 100  $\mu\text{a}$  and 140  $\mu\text{a}$  (both for different values of the high-frequency cutoff and for direct feed into the oscilloscope). These photographs are shown in Figs. 19 and 20 together with the Pearson curves calculated for the values of the skewness and excess obtained with these currents and spectra. The general trend toward a gaussian distribution as the high-frequency limit is decreased can be seen from these curves, the approach being faster

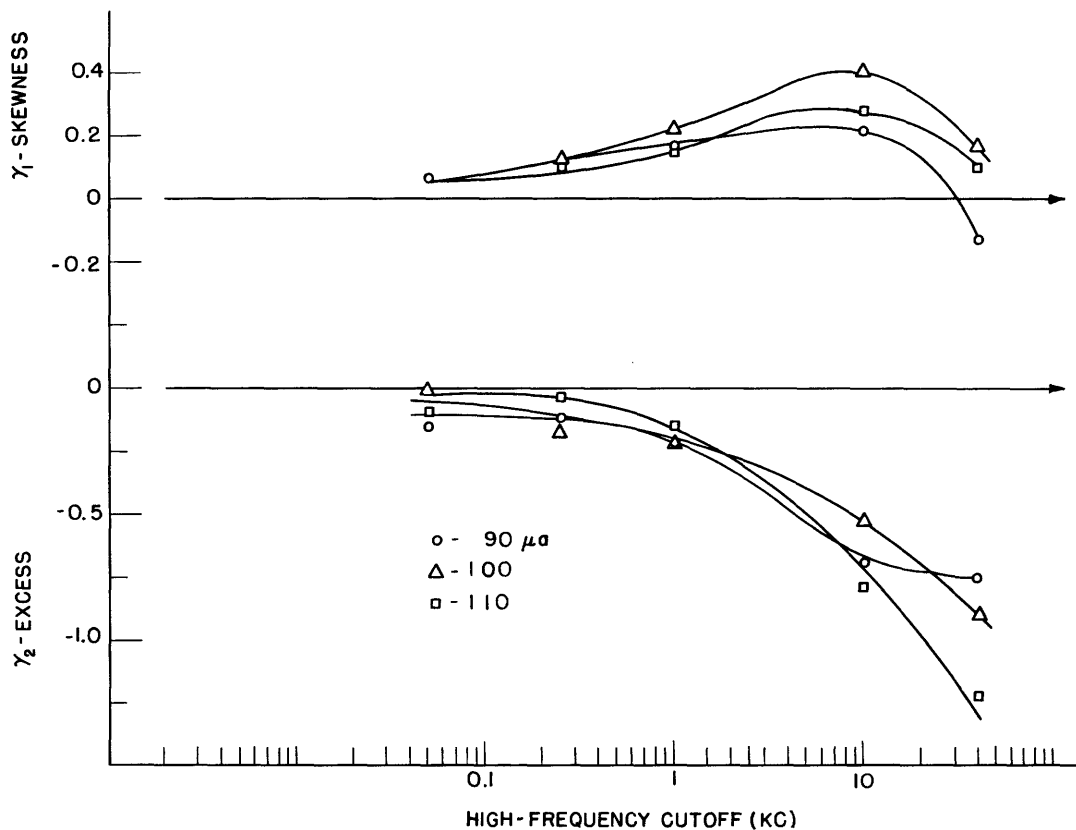


Fig. 16. Effect of high-frequency cutoff on measured values of skewness and excess for inverse currents of 90, 100, and 110  $\mu\text{a}$ .

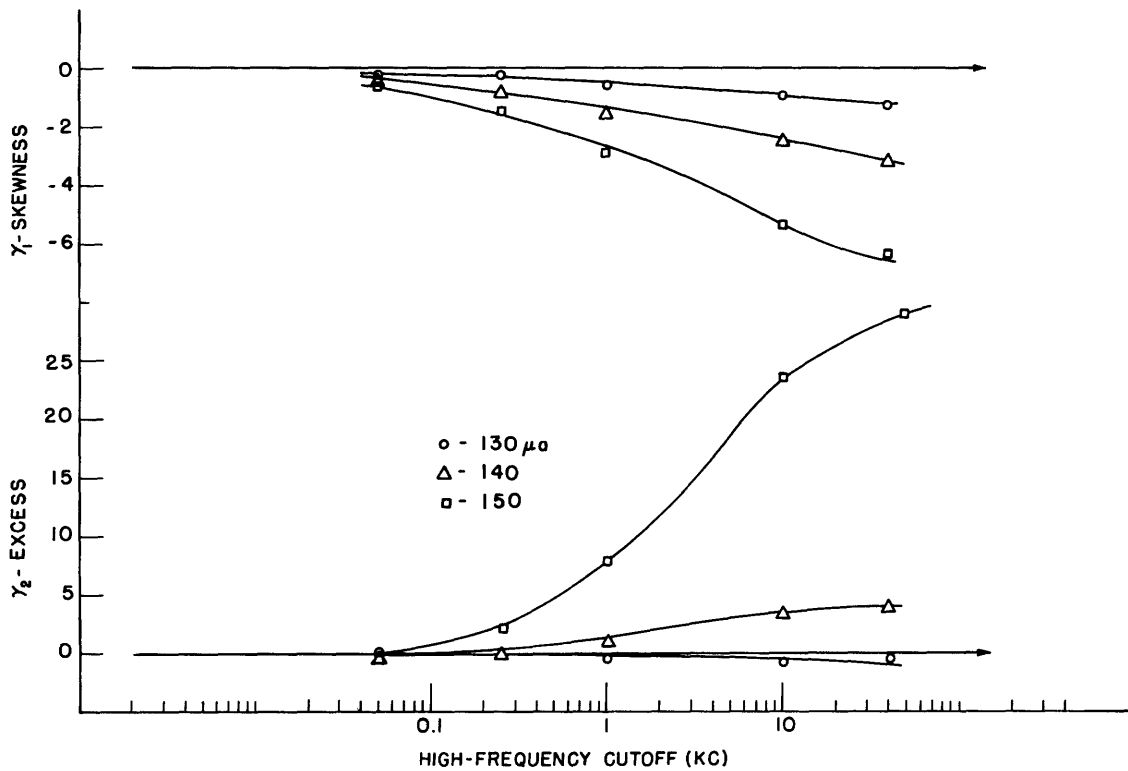


Fig. 17. Effect of high-frequency cutoff on measured values of skewness and excess for inverse currents of 130, 140, and 150  $\mu a$ .

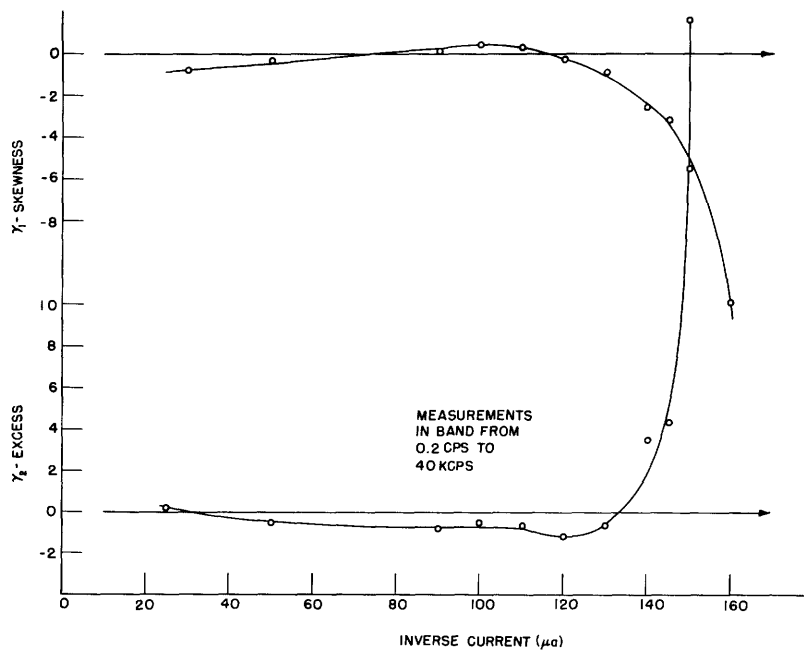


Fig. 18. Variation of the skewness and excess of avalanche noise with inverse current.

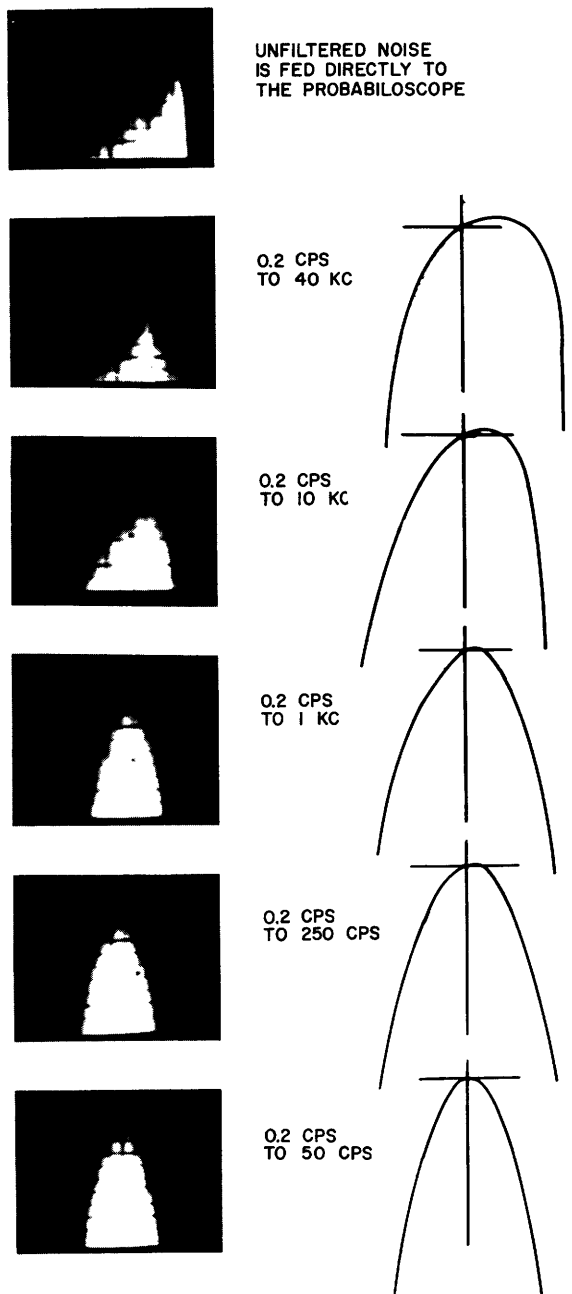


Fig. 19. Probabiloscope photographs and Pearson curves for  $100\text{-}\mu\text{a}$  avalanche noise examined with different system bandwidths.

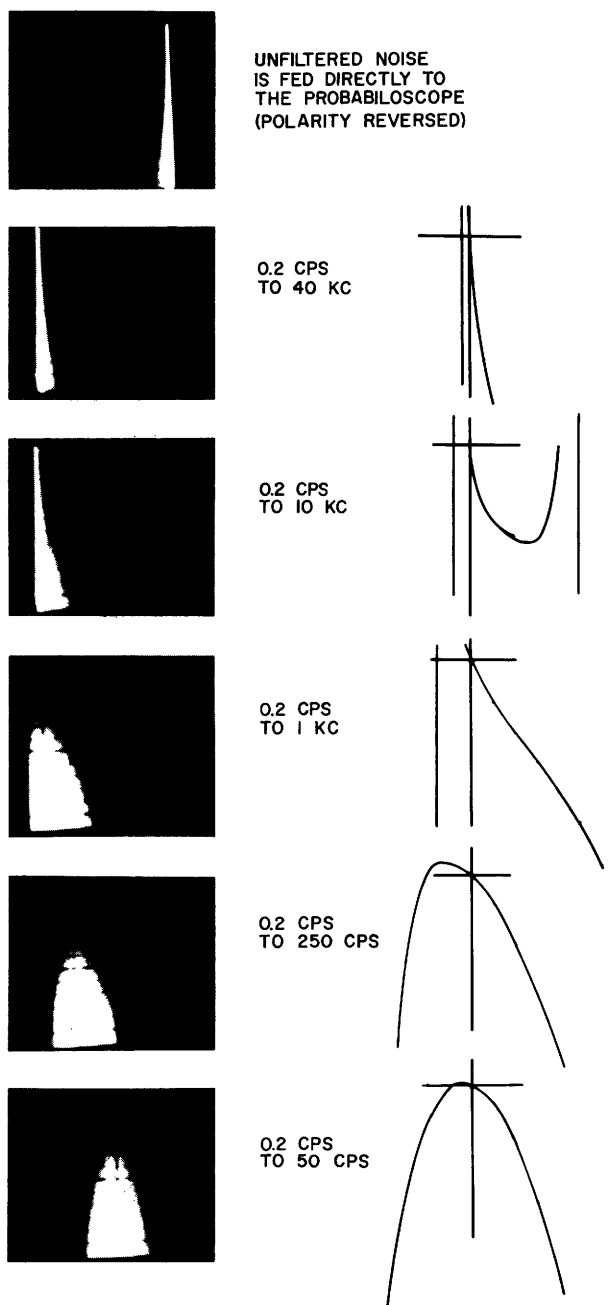


Fig. 20. Probabiloscope photographs and Pearson curves for  $140\text{-}\mu\text{a}$  of inverse current (avalanche noise) examined for different system bandwidths.

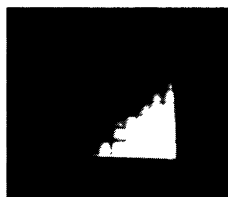
for a distribution with a wide range of values (as for  $100\mu\text{a}$ ) than for a distribution that is almost discrete in nature (as for  $140\mu\text{a}$ ). These curves also illustrate some shortcomings of the Pearson system. In the 0.2 cps - 0.40 kc curve of Fig. 19 the rather irregular distribution shown in the probabioscope photograph is poorly approximated. More serious is the poor approximation shown in Fig. 20 to the case in which the system bandwidth is 0.2 cps to 10 kc. Although further investigation shows that almost 90 per cent of the area under the distribution density curve is in the left-hand maximum, the presence of the second peak as a result of the Pearson assumptions is quite undesirable. This emphasizes the desirability of having available a qualitative probabioscope curve when applying the Pearson system. The modification of the distribution in Fig. 19, even for a system bandwidth from 0.2 cps to 40 kc, is also worth noting.

In addition, probabioscope photographs were taken for several values of reverse current, using direct feed to the oscilloscope. These curves (Fig. 21) show quite clearly the increasing probability of one amplitude level as the inverse current is increased.

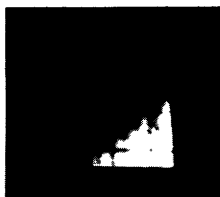
The interpretation of the curves is greatly aided by examination of the actual waveforms.

The waveform photographs in Fig. 22 show how the approach to a gaussian distribution takes place: that is, the sharp pulses of the avalanche noise are averaged so that we see fluctuations in the density of pulses rather than the pulses themselves. The waveform photographs for several values of inverse current shown in Fig. 23 were taken by feeding the noise directly to a Tektronix 535 oscilloscope. They are helpful in interpreting the probabioscope photographs of Fig. 21. They show that avalanche noise consists of a series of nonoverlapping pulses whose density decreases as the current increases.

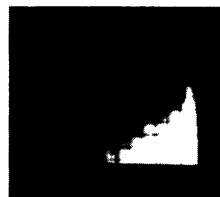
This investigation illustrates that frequently photographs of waveforms yield more information about the process than a probability distribution. If, however, probability distributions are desired, when the correlation time for the process is short, as for avalanche noise, a direct probability analyzer would provide more precise information about the distribution than a moments-measuring analyzer. In this connection, a system bandwidth wider than that employed here is probably necessary for the accurate evaluation of the probability density of a process like avalanche noise, whose waveform consists of rapid transitions between states. Thus the avalanche noise investigation has clearly shown some of the shortcomings of the moments-measuring method, in addition to demonstrating the ease of handling data in the form of moments.



27 MICROAMPERES



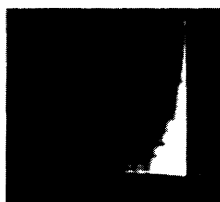
50 MICROAMPERES



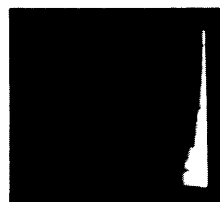
90 MICROAMPERES



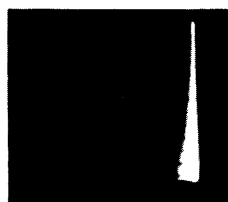
100 MICROAMPERES



110 MICROAMPERES



120 MICROAMPERES



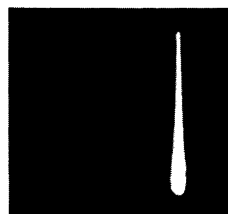
130 MICROAMPERES



140 MICROAMPERES



145 MICROAMPERES



150 MICROAMPERES



160 MICROAMPERES

Fig. 21. Probabiloscope photographs of unfiltered avalanche noise for various inverse currents.

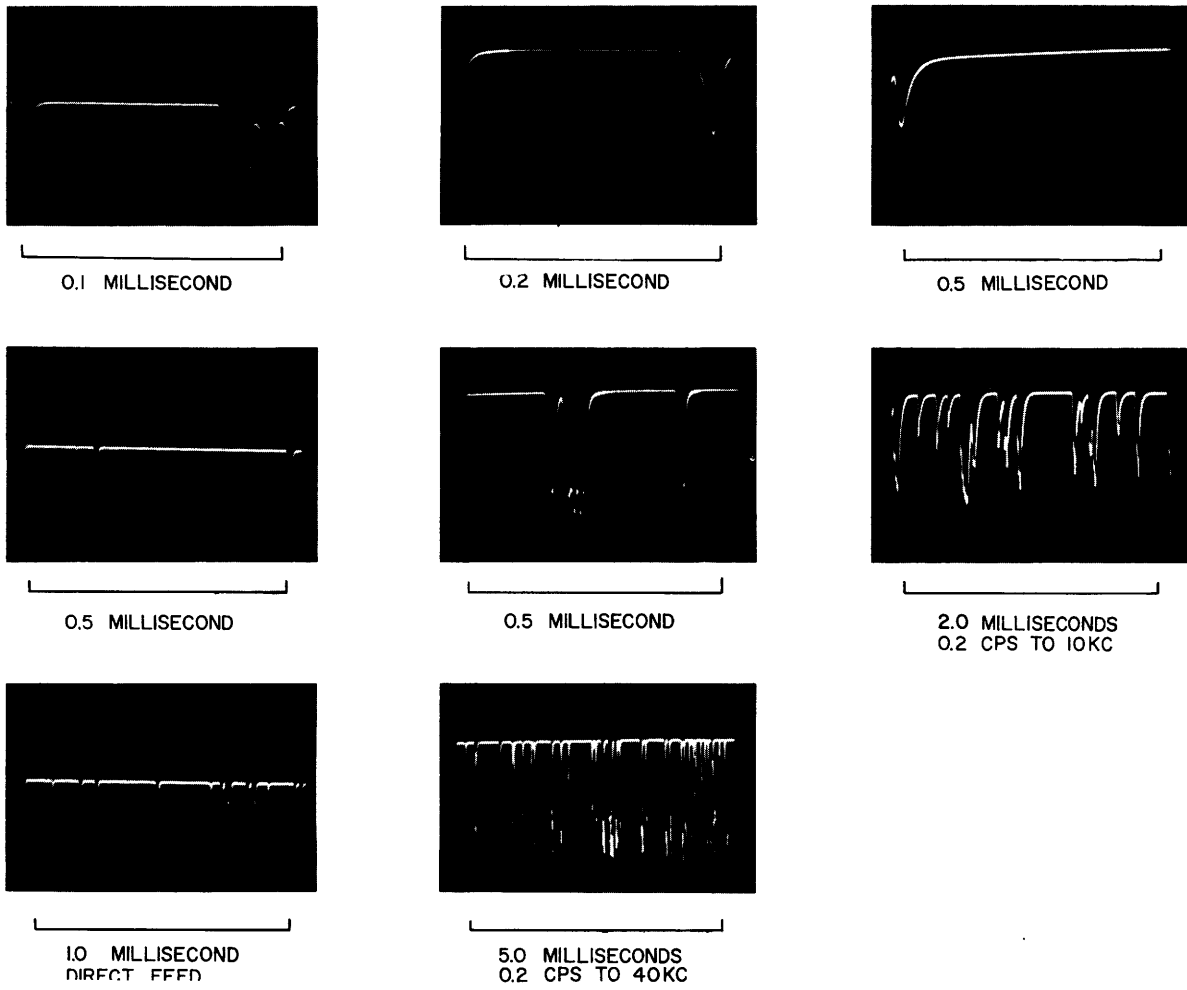
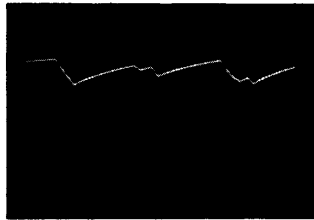
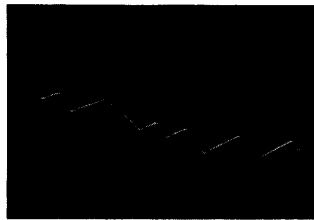


Fig. 22(a). Effect of filtering on the waveform of avalanche noise ( $140 \mu a$ ).

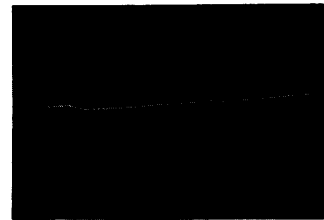




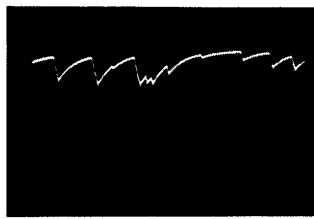
0.5 MILLISECOND



0.5 MILLISECOND



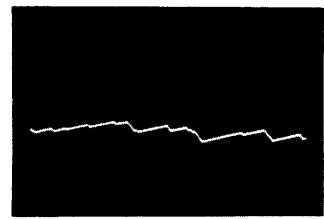
0.5 MILLISECOND



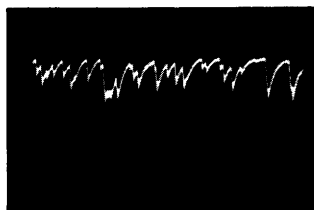
2.0 MILLISECONDS



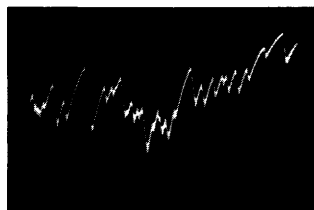
2.0 MILLISECONDS



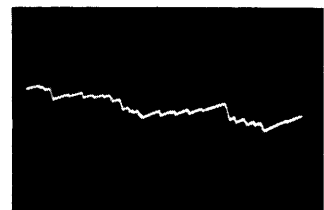
2.0 MILLISECONDS



5.0 MILLISECONDS  
0.2 CPS TO 1KC



5.0 MILLISECONDS  
0.2 CPS TO 250 CPS



5.0 MILLISECONDS  
0.2 CPS TO 50 CPS

Fig. 22(b). Effect of filtering on the waveform of avalanche noise ( $140 \mu a$ ).

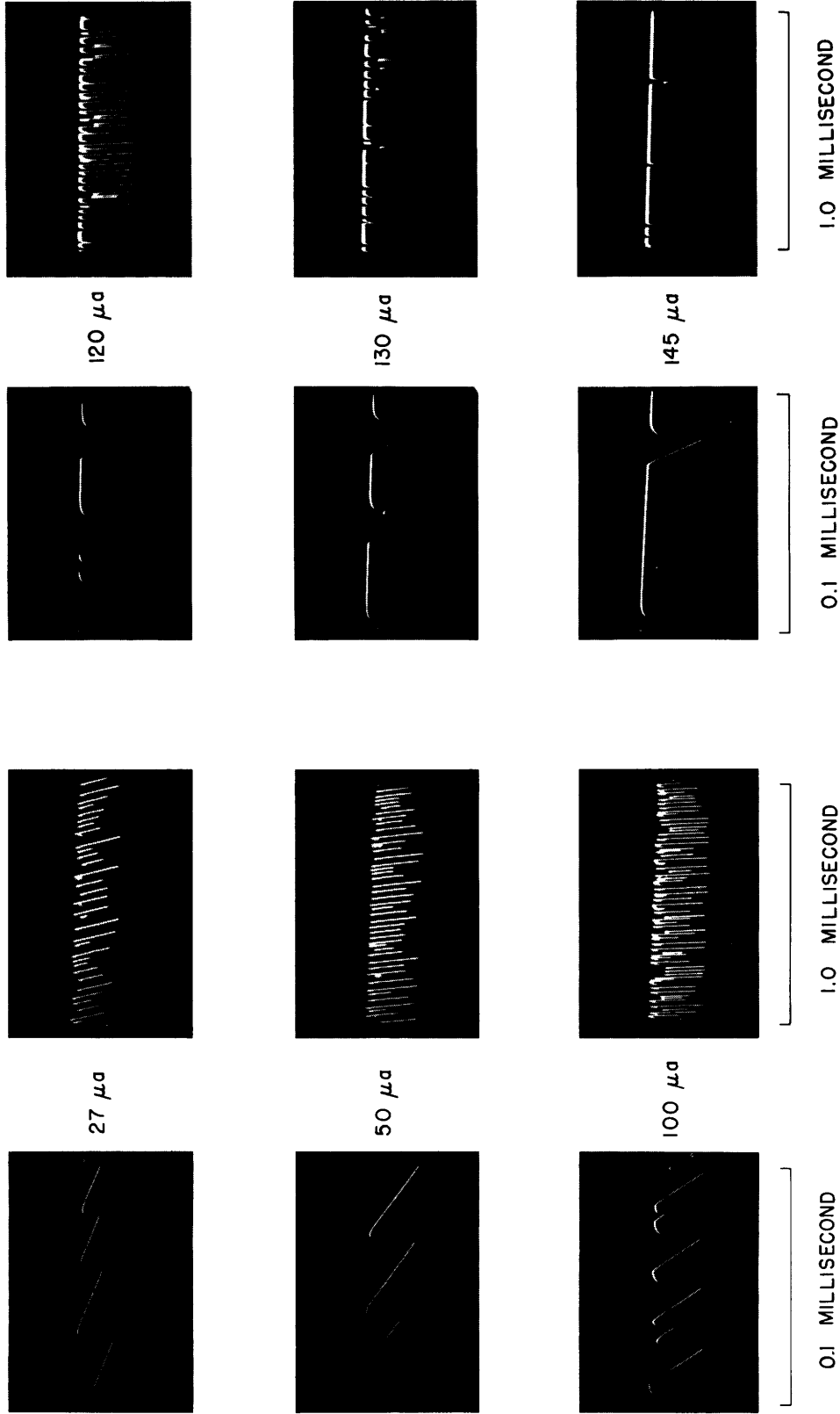


Fig. 23. Avalanche noise waveforms for several values of inverse current.

## V. CONCLUSIONS

We have attempted to describe a moments technique that is useful in the experimental investigation of physical noises, and in the analysis of the effects of networks on such noises.

The moments technique provides a theoretical tool of great usefulness in the examination of the effect of filters through an amplitude distribution for several classes of non-gaussian noise. Specifically, when the higher-order autocorrelation functions or spectral densities of these noises are obtainable, and when the frequency response of the network is easily handled analytically, in the frequency domain the moments technique can be employed. On the other hand when the random-pulse type of non-gaussian noise is considered, and the impulse response of the filter is simple, the moments-measuring technique in the time domain is attractive. Here, for example, we have considered the nature of the approach of a random-pulse noise model to a gaussian distribution for severe band-limiting, with special attention to the behavior of the higher-order moments.

We have also examined the effect of an RC limited bandwidth filter on random-pulse noise. All noises are inherently non-gaussian (in the strictest sense), since they consist of effects that are quantized; but the measuring system is usually not capable of distinguishing these discrete events. Middleton (4) suggested the basic idea that it is the overlap of large numbers of pulses which leads to an essentially gaussian distribution. In this work we have elaborated this conclusion by showing that the overlap caused by the filtering action of the measuring system itself must be considered in evaluating the validity of the measured distribution parameters that are obtained from such a system. More specifically, we have indicated that the "memory" of the measuring system has the most important role in modifying the distribution.

The experimental application of a moments technique is of particular value when  $1/f$  noise, for which the correlation time is long, is being examined. The limiting factor in any measurement of the probability density is the length of observation time. For direct probability density measurements, this both limits the accuracy and requires equipment capable of making simultaneous multilevel measurements on the tails of the distribution. In such a case, measurement of the moments, and application of Pearson's system to obtain a suitable curve, provide a considerable saving of equipment. A moments technique is particularly applicable when it is desirable (and sufficient) to characterize a distribution by a small number of parameters, as is the case when the deviation of a distribution from gaussian is being examined.

Such was the case in the measurement of moments of  $1/f$  noise. Bell (30) had previously made direct measurements of the distribution of carbon resistor noise in a frequency band from 40 cps to 6 kc. In this investigation we felt it desirable to make measurements in a wider band and to get a direct characterization of the departure

from gaussian, if any. Our conclusion is that, since the deviation from gaussian lies within the experimental error, the  $1/f$  noise has a first-probability distribution which can be characterized as gaussian.

The measurement of the moments of the avalanche noise, however, illustrates the shortcomings of an approach that gives attention exclusively to measuring the moments. For such a noise (where there is a short correlation time), it is feasible to make accurate direct measurements of the distribution density. From these measurements, the skewness and excess can then be calculated to characterize the departure from gaussian statistics. It is clear, also, that a bandwidth greater than 10 kc is desirable for noises with flat or nearly flat spectra going to higher frequencies. This is very difficult to achieve with the desired high accuracy with the type of function generator used here.

#### Acknowledgment

The author wishes to express his appreciation to Professor Richard B. Adler for his guidance and encouragement throughout the last three years. He also acknowledges many helpful discussions of the instrumentation problems with Bradford Howland, Robert M. Brown, and Julian G. Ingersoll. The assistance of Mrs. Catherine S. Aborjaily, who built a great deal of the equipment, must be singled out for special praise.

## APPENDIX

### Further Applications of the Moments Approach in the Time Domain


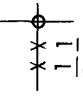
Values for the moments of the output from linear systems whose input is random-pulse noise were obtained in a number of cases, in addition to the one described in section 2.3. These results are tabulated below.

In Table A-1 we consider the response to randomly distributed unit steps; in Table A-2, the response to unit pulses of length  $r$  seconds.

The average density of pulses is assumed to be  $\bar{N}$  pulses/second. The values for the  $n^{\text{th}}$ -order semi-invariants and for the skewness and excess are tabulated directly. The moments values can easily be obtained from the semi-invariants (16).

Table A-1. Semi-Invariants of the Output for Random Unit Steps Incident on the Network H(s) and Some Expressions for the Skewness and Excess.					
H(s)	Poles and Zeros in the s-plane	$K_n/\bar{N}$	$\gamma_1$	$\gamma_2$	
$\frac{s}{s + \frac{1}{r}}$		$\frac{r}{n}$	$\frac{1}{\sqrt{\frac{9}{8} \bar{N} r}}$	$\frac{1}{\bar{N} r}$	
$\frac{s}{r_0(s + \frac{1}{r_0})(s + \frac{1}{r})}$		$\frac{(-1)^m}{(m-l)! l!} \sum_{l=0}^m \frac{r r_0}{(m-l) r_0 + l r}$	$\frac{1}{\sqrt{\bar{N} \frac{3(r_0 + 2r)(r + 2r_0)}{4\sqrt{2}(r + r_0)^{3/2}}}}$	$\frac{1}{\bar{N} \frac{(3r_0 + r)(r_0 + 3r)}{3(r_0 + r)}}$	
$\frac{s}{(s+a)^2 + \omega_0^2}$			$\frac{1}{\sqrt{\bar{N} \frac{3(9a^2 + \omega_0^2)}{16\sqrt{a^2 + \omega_0^2} a^{3/2}}}}$	$\frac{1}{\bar{N} \frac{2(4a^2 + \omega_0^2)}{3a(a^2 + \omega_0^2)}}$	
$\frac{s(s+a_0)}{(s+a)^2 + \omega_0^2}$			$\frac{1}{\sqrt{\bar{N} \frac{3(9a^2 + \omega_0^2)(a_0^2 + a^2 + \omega_0^2)^{3/2}}{16a^{3/2} \sqrt{a^2 + \omega_0^2} [2(a_0 - a)^3 + 6a(a_0 - a)^2 + 9a^2 a_0 + 4a\omega_0^2 + 3a_0\omega_0^2]}}}$		
$\frac{s}{(s+a)^m}$		$\frac{[n(m-1) + 1]!}{[(m-1)!]^n (na)^{[n(m-1)+1]}}$	$\frac{1}{\sqrt{\bar{N} (\frac{3}{2})^{3m-(3/2)} \frac{[(2m-1)!]^{3/2}}{\sqrt{3a(3m-2)!}}}}$	$\frac{1}{\bar{N} \frac{[(2m-1)!]^2}{8a(4m-3)!}}$	

Table A-2. Semi-Invariants of the Output for Random Unit Pulses of Duration  $r$  Incident on the Network  $H(s)$ .

$H(s)$	Poles and Zeros in the $s$ -plane	$K_n/\bar{N}$	$\gamma_1$	$\gamma_2$
$\frac{s}{s + \frac{1}{r}}$		$\frac{r}{n} [1 - e^{-nr/r} + (1 - e^{-r/r})^n]$	$\frac{1}{\sqrt{N} \sqrt{\frac{9}{8} r [1 - e^{-2r/r} + (1 - e^{-r/r})^2]^{3/2}}}$	$\frac{1}{\bar{N} r \frac{[1 - e^{-2r/r} + (1 - e^{-r/r})^2]^2}{[1 - e^{-4r/r} + (1 - e^{-r/r})^4]}}$
$\frac{s}{r_0 (s + \frac{1}{r_0})(s + \frac{1}{r})}$		$\left(\frac{r}{r-r_0}\right)^n \sum_{\ell=0}^n \frac{(-1)^\ell n!}{(n-\ell)! \ell!} \frac{r r_0}{(n-\ell) r_0 + \ell r} \times [1 - e^{-(n-\ell)/r + (\ell/r_0)r} + (e^{r/r} - 1)^{n-\ell} (e^{-r/r_0} - 1)^\ell]$		

## BIBLIOGRAPHY

1. A. Van der Ziel, Noise (Prentice-Hall, Inc. , New York, 1954), p. 2.
2. S. O. Rice, Mathematical analysis of random noise, Bell System Tech. J. 23, 282 (1944); 24, 46 (1945); W. R. Bennett, Response of a linear rectifier to signal and noise, J. Acoust. Soc. Am. 15, 164 (1944); D. Middleton, The response of biased, saturated linear, and quadratic rectifiers to random noise, J. Appl. Phys. 17, 778 (1946); Some general results in the theory of noise through nonlinear devices, Quart. Appl. Math. 5 (Jan. 1948); W. R. Bennett, The biased ideal rectifier, Bell System Tech. J. 26, 139 (1947).
3. M. Kac and A. J. F. Siegert, On the theory of noise in radio receivers with square law detectors, J. Appl. Phys. 18, 383 (April 1947).
4. S. O. Rice, Mathematical analysis of random noise, Bell System Tech. J. 23, 282 (1944); 24, 46 (1945); D. Middleton, On the theory of random noise: Phenomenological models I, II, J. Appl. Phys. 22, 1143 (Sept. 1951).
5. R. Furth and D.K.C. MacDonald, Statistical analysis of spontaneous electrical fluctuations, Proc. Phys. Soc. (London) 59, 388-403 (1947); Quarterly Progress Report, Research Laboratory of Electronics, M.I.T. , Jan. 15, 1948, p. 51.
6. N. Knudtson, Experimental study of statistical characteristics of filtered random noise, Technical Report 115, Research Laboratory of Electronics, M.I.T. , July 15, 1949; W. B. Davenport, Jr., J. Acoust. Soc. Am. 24, 390-399 (1952); E. R. Kretzmer, Statistics of television signals, Bell System Tech J. 31, 751-763 (1952); L. W. Orr, Wide band amplitude distribution analysis of voltage sources, Rev. Sci. Instr. 25, 894-898 (1954).
7. H. Cramér, Mathematical Methods of Statistics (Princeton University Press, Princeton, 1951), p. 221.
8. W. P. Elderton, Frequency Curves and Correlation (Harren Press, Washington, 4<sup>th</sup> ed. , 1953).
9. J. Hilibrand, Sc.D. Thesis, Department of Electrical Engineering, M.I.T. , Aug. 1956.
10. I. A. Mullen and D. Middleton, Rectification of nearly gaussian noise, Technical Report 189, Cruft Laboratory, Harvard University, 1954.
11. B. Mazelsky, Extension of power spectral methods of generalized harmonic analysis to determine non-gaussian probability functions of random input disturbances and output responses of linear systems, J. Aero. Sci. 21, 145-153 (March 1954).



12. W. B. Davenport, Jr. and W. L. Root, Introduction to Noise Theory (McGraw-Hill Book Company, Inc. , New York, to be published), Chap. 10.
13. A. B. MacNee, An electronic differential analyzer, Proc. IRE 37, 1315-1324 (1949).
14. D. Middleton, On the theory of random noise: phenomenological models I, II, J. Appl. Phys. 22, 1143 (1951).
15. H. Cramér, op. cit. , p. 204.
16. Ibid. , p. 185.
17. Ibid. , p. 187.
18. Ibid. , p. 213.
19. Ibid. , p. 183.
20. Vacuum Bottles, Consumers Union Reports, July 1954, p. 325.
21. D. I. Kosowsky, S.M. Thesis, Department of Electrical Engineering, M. I. T. , 1952.
22. R. F. Kemp, Cathode ray oscilloscope intensity modulator, Rev. Sci. Instr. 26, 1120-1121 (1955).
23. E. R. Kretzmer, loc. cit.
24. J. P. Costas, Periodic sampling of stationary time series, Technical Report 156, Research Laboratory of Electronics, M. I. T. , May 16, 1950.
25. W. B. Davenport, Jr. , R. A. Johnson, and D. Middleton, Statistical errors in measurements on random time functions, J. Appl. Phys. 23, 337-388 (April 1952).
26. A. J. F. Siegert, J. Appl. Phys. 23, 737-742 (1952).
27. E. Jahnke and F. Emde, Tables of Functions (Dover Publications, New York, 4<sup>th</sup> ed. , 1945), p. 4.
28. W. Flügge, Four Place Tables of Transcendental Functions (McGraw-Hill Book Company, Inc. , 1954), p. 115.
29. K. G. McKay, Avalanche breakdown in silicon, Phys. Rev. 94, 877-884 (1954); K. G. McKay and K. B. McAfee, Electron multiplication in silicon and germanium, Phys. Rev. 91 (1953).
30. D. A. Bell, Distribution function of semiconductor noise, Proc. Phys. Soc. (London) 68, 690 (1955).

